Biogeosciences Discuss., doi:10.5194/bg-2016-52, 2016
Manuscript under review for journal Biogeosciences
Published: 16 February 2016

Biogeosciences Discussions
Open Access
EGU

Microbial dynamics in a High-Arctic glacier forefield: a combined field, laboratory, and modelling approach.

James A. Bradley [1,2], Sandra Arndt [2], Marie Šabacká [1], Liane G. Benning [3,4], Gary L. Barker [5], Joshua J. Blacker [3], Marian L. Yallop [5], Katherine E. Wright [1], Christopher M. Bellas [1], Jonathan Telling [1], Martyn Tranter [1], Alexandre M. Anesio [1]

[1] Bristol Glaciology Centre, School of Geographical Sciences, University of Bristol, BS8 1SS, UK
[2] BRIDGE, School of Geographical Sciences, University of Bristol, BS8 1SS, UK
[3] School of Earth and Environment, University of Leeds, LS2 9JT, UK
[4] GFZ, German Research Centre for Geosciences, 14473 Potsdam, Germany
[5] School of Biological Sciences, University of Bristol, BS8 1SS, UK

Corresponding author: James A. Bradley, email: j.bradley@bristol.ac.uk

Abstract: Modelling the development of soils in glacier forefields is necessary in order to assess how microbial and geochemical processes interact and shape soil development in response to glacier retreat. Furthermore, such models can help us predict microbial growth and the fate of Arctic soils in an increasingly ice-free future. Here, for the first time, we combined field sampling with laboratory analyses and numerical modelling to investigate microbial community dynamics in oligotrophic proglacial soils in Svalbard. We measured low bacterial growth rates and growth efficiencies (relative to estimates from Alpine glacier forefields), and high sensitivity to soil temperature (relative to temperate soils). We used these laboratory measurements to inform parameter values in a new numerical model and significantly refined predictions of microbial and biogeochemical dynamics of soil development over a period of roughly 120 years. The model predicted the observed accumulation of autotrophic and heterotrophic biomass. Genomic data indicated that initial microbial communities were dominated by bacteria derived from the subglacial environment, whereas older soils hosted a mixed community of autotrophic and heterotrophic bacteria. This finding was validated by the numerical model, which showed that active microbial communities play key roles in fixing and recycling carbon and nutrients. We also demonstrated the role of allochthonous carbon and microbial necromass in sustaining a pool of organic material, despite high heterotrophic activity in older soils. This combined field, laboratory and modelling approach demonstrates the value of integrated model-data studies to understand and quantify the functioning of the microbial community in an emerging High-Arctic soil ecosystem.

Key words
Glacier forefield
Microbial dynamics
Soil development
Numerical modelling
Integrated field-laboratory-modelling

Biogeosciences Discuss., doi:10.5194/bg-2016-52, 2016
Manuscript under review for journal Biogeosciences
Published: 16 February 2016

1. Introduction

Polar regions are particularly sensitive to anthropogenic climate change (Lee, 2014) and have experienced accelerated warming in recent decades (Johannessen et al., 2004; Serreze et al., 2000; Moritz et al., 2002). The response of terrestrial Polar ecosystems to this warming is complex. Warmer conditions may increase soil respiration contributing to a positive feedback effect resulting from an increase in CO_2 efflux to the atmosphere. This will lead to further warming induced by the greenhouse effect (Billings, 1987; Oechel et al., 1993; Goulden et al., 1998). However, Arctic soils in particular may over several decades acclimatize to warming due to an increase in primary productivity, generating a net sink of CO_2 during the summer (Oechel et al., 2000). Accordingly, research to understand the response of terrestrial ecosystems in high latitudes to environmental change is of increasing importance. A visible consequence of Arctic warming is the large-scale retreat of glacier and ice cover (ACIA, 2005; Paul et al., 2011; Staines et al., 2014; Dyurgerov and Meier, 2000). From underneath the ice, a new terrestrial biosphere emerges, playing host to an ecosystem which may exert an important influence on biogeochemical cycles, and more specifically atmospheric CO_2 concentrations and associated climate feedbacks (Dessert et al., 2003; Anderson et al., 2000; Smittenberg et al., 2012; Berner et al., 1983). Furthermore, such a dramatic change will also invariably affect global methane budgets (Kirschke et al., 2013), the phosphorus cycle (Filippelli, 2002; Follmi et al., 2009) and the productivity of downstream and coastal ecosystems (Anesio et al., 2009; Mindl et al., 2007; Fountain et al., 2008; Anderson et al., 2000).

Numerous studies have attempted to characterize the physical and biological development of recently exposed soils using a chronosequence approach, whereby a transect perpendicular to the retreating ice snout represents a time sequence with older soils at increasing distance from the ice snout (Schulz et al., 2013). We have recently shown that microbial biomass and macronutrients (such as carbon, phosphorus and nitrogen) can accumulate in soils over timescales of decades to centuries (Bradley et al., 2014). In such pristine glacial forefield soils the activity of microbial communities is thought to be responsible for this initial accumulation of carbon and nutrients. Such an accumulation facilitates colonization by higher order plants, leading to the accumulation of substantial amounts of organic carbon (Insam and Haselwandter, 1989). However, organic carbon may also be derived from allochthonous sources such as material deposited on the soil surface (from wind, hydrology, precipitation and ornithogenic sources) and ancient organic pools derived from under the glacier (Schulz et al., 2013). Nevertheless, the relative significance of allochthonous and autochthonous sources of carbon to forefield soils, as well as their effect on ecosystem behavior are so far still poorly understood (Bradley et al., 2014). Moreover, cycling of bioavailable nitrogen (which is derived from active nitrogen-fixing organisms, allochthonous deposition, and degradation of organic substrates) and phosphorus (liberated from the weathering of minerals and decomposition of organic substrates) are similarly poorly quantified.

Several studies have observed shifts in the microbial community inhabiting pro-glacial soils of various ages (Zumsteg et al., 2012; Zumsteg et al., 2011). This was expressed in increasing rates of

Biogeosciences Discuss., doi:10.5194/bg-2016-52, 2016
Manuscript under review for journal Biogeosciences
Published: 16 February 2016

autotrophic and bacterial production with soil age (Schmidt et al., 2008; Zumsteg et al., 2013; Esperschutz et al., 2011; Frey et al., 2013) and the overall decline in quality of organic substrates in older soils (Goransson et al., 2011; Insam and Haselwandter, 1989). However, current evidence is limited to mostly descriptive approaches, which may be challenging to interpret due to inherent difficulties in disentangling interacting microbial and geochemical processes across various temporal and spatial scales. Furthermore, the inherent heterogeneity of glacial forefield soils makes the development of a single conceptual model that fits all challenging. Accordingly, pro-glacial biogeochemical processes that dominate such systems remain poorly quantified and highly under-explored. This current lack of understanding limits our ability to predict the future evolution of these emerging landscapes and the potential consequences on global climate. Numerical models present an opportunity to expand our knowledge of glacier forefield ecosystems by analytically testing the hypotheses that arise from observations, extrapolating, interpolating and budgeting processes, rates and other features to explore beyond the possibility of empirical observation (Bradley et al., 2016). With such a model we can then also explore the sensitivity and resilience of these ecosystems to environmental change.

To address this, we have combined field observations, with laboratory incubations and elemental measurements as well as genomic analyses and used these in a numerical model to investigate the development of soils in a glacial forefield. With this data we refined some model parameters in the recently developed ***S***oil biogeoc***H***em***I***cal ***M***odel for ***M***icrobial ***E***cosystem ***R***esponse (SHIMMER 1.0; Bradley et al. (2015)) model and applied this to the emerging forefield of the Midtre Lovénbreen glacier in Svalbard. The Midtre Lovénbreen forefield is an ideal site to test the field-laboratory-model approach due to the lack of vegetation during the first century of soil development, as this would obscure the microbial community dynamics and considerably alter the physical properties of the soil (Brown and Jumpponen, 2014; Ensign et al., 2006; King et al., 2008; Kastovska et al., 2005; Schutte et al., 2009; Duc et al., 2009). The model development was informed by decades of empirical research on glacier forefield soils, and has already been tested and validated using published datasets from the Damma Glacier in Switzerland and the Athabasca Glacier in Canada. A thorough sensitivity analysis highlighted the most important parameters to constrain in order to make further predictions more robust. All our model parameter values are specific to individual, local model conditions and inherently contain necessary model simplifications, abstractions and assumptions. Nevertheless, our earlier sensitivity analyses revealed the following highly sensitive key parameters as the most important to constrain through measurements: the maximum heterotrophic growth rate (I_{maxH}), the bacterial growth efficiency (BGE, parameter Y_H) and the temperature response (Q_{10}). Therefore, in this current study, we combined detailed field measurements with specifically designed laboratory experiments and quantified values for these three parameters with a specific set of soils from for the Midtre Lovénbreen forefield. With this data we have improved the confidence in our model predictions and assessed the model performance. Finally, the model was used to explore microbial community structure and carbon cycling dynamics in this High Arctic setting.

Biogeosciences Discuss., doi:10.5194/bg-2016-52, 2016
Manuscript under review for journal Biogeosciences
Published: 16 February 2016

2. Methods

2.1. Study site and sampling

Midtre Lovénbreen is an Arctic polythermal valley glacier on the south side of Kongsfjorden, Western Svalbard (latitude 78°55'N, longitude 12°10'E) (Fig. 1). The Midtre Lovénbreen catchment is roughly 5 km East of Ny-Ålesund, where several long-term monitoring programs have provided a wealth of contextual information. Midtre Lovénbreen has experienced negative mass balance throughout much of the 20th century. Since the end of the Little Ice Age (maximum in Svalbard in the 1900s) the de-glaciated surface area of the Midtre Lovénbreen catchment has increased considerably in response to warming mean annual temperatures. This continues to the present day. Between 1966 and 1990 ~ 2.3 km^2 of land was exposed (Fleming et al., 1997; Moreau et al., 2008). We used a chronosequence approach to determine ages for soils based on satellite imagery (Landsat TM 7) and previously determined soil ages by aerial photography and carbon-14 dating techniques in Hodkinson et al. (2003). Soil samples were collected along a transect perpendicular to the glacier snout, representing soil ages of 0, 3, 5, 29, 50, and 113 years (Fig. 1) during the field season (18 July to 29 August 2013). At each of the 6 sites along the chronosequence, 10 meter traverses roughly parallel to the glacier snout were established and at each site 3 soil plots were sampled (using ethanol sterilized sampling equipment). After removing the > 2 cm rock pieces at each site, about 100 grams of soil was collected from the top 15 cm and immediately placed into sterile high-density polyethylene bags (Whirl-Pak (Lactun, Australia)) that were frozen and stored at -20°C, and transported to the laboratories in the Universities of Bristol and Leeds (UK).

2.2. Laboratory analyses

For bacterial abundance, samples were thawed and aliquots (100 mg) were immediately transferred into sterile 1.5 mL micro-centrifuge (Eppendorf) tubes, where they were diluted with 900 µL of Milli-Q water (0.2 µm filtered) and immediately fixed in 100 µL glutaraldehyde (0.2 µm filtered, 2.5% final concentration). Samples were then vortexed for 10 seconds and sonicated for 1 minute at 30°C to facilitate cell detachment from soil particles. Ten µL fluorochrome DAPI (4', 6-diamidino-2 phenylindole) was added to half of the samples, tubes were vortexed briefly (3 seconds) and incubated in the dark for 10 minutes, to be counted under UV light. The other half of each sample remained untreated, for counting under auto-fluorescent light for photosynthetic pigmentation. Samples were vortexed for 10 seconds and let stand for a further 30 seconds to ensure a well-mixed solution, prior to filtering 100 µL of the mixed liquid sample onto black Millipore Isopore membrane filters (0.2 µm pore size, 25 mm diameter), rinsed with a further 250 µL of Milli-Q water (0.2 µm filtered). Bacterial cells were then counted using an Olympus BX41 microscope at 1000 times magnification. The filtering apparatus was washed out with Milli-Q water between each filtration, and negative control samples, prepared using Milli-Q water, were included into each series. A negative control was a sample with no visible stained or auto-fluorescing cells. Thirty random grids (each 10^4 µm^2) were counted per sample. Cell morphologies were measured and cell volume was estimated and converted to carbon content according to Bratbak and Dundas (1984) (see Supplementary

Biogeosciences Discuss., doi:10.5194/bg-2016-52, 2016
Manuscript under review for journal Biogeosciences
Published: 16 February 2016

Information). Separate aliquots of soil from each site were weighed after thawing and then dried at 105°C to obtain an estimate of soil moisture content.

Environmental DNA was isolated from at least 3 replicates for each soil age using MoBio PowerSoil® DNA Isolation Kit and by following the instruction manual. The isolated 16S rDNA was amplified with bacterial primers 515f (5'-GTGYCAGCMGCCGCGGTAA-3') and 926r (5'-CCGYCAATTYMTTTRAGTTT-3'), creating a single amplicon of ~400 bp. The reaction was carried out in 50 µL volumes containing 0.3 mg mL^{-1} Bovine Serum Albumin, 250 µM dTNPs, 0.5 µM of each primer, 0.02 U Phusion High-Fidelity DNA Polymerase (Finnzymes OY, Espoo, Finland) and 5x Phusion HF Buffer containing 1.5 mM $MgCl_2$. The following PCR conditions were used: initial denaturation at 95°C for 5 minutes, followed by 25 cycles consisting of denaturation (95°C for 40 seconds), annealing (55°C for 2 minutes) and extension (72°C for 1 minute) and a final extension step at 72°C for 7 minutes. Samples were sequenced using the Ion Torrent platform (using Ion 318v2 chip) at Bristol Genomics facility at the University of Bristol. A non-barcoded library was prepared from the amplicon pool using Life technologies Short Amplicon Prep Ion Plus Fragment Library Kit. The template and sequencing kits used were: Ion PGM Template OT2 400 Kit and Ion PGM Sequencing 400 kit. The sequencing yielded 4.38 million reads. The 16S sequences were further processed using MOTHUR (v. 1.35) and QIIME pipelines (Schloss et al., 2009; Caporaso et al., 2010). Chimeric sequences were identified and removed using UCHIME (Edgar et al., 2011) and reads were clustered into operational taxonomical units (OTUs), based on at least 97% sequence similarity, and assigned taxonomical identification against Greengenes bacterial database (McDonald et al., 2012).

The carbon contents in the year 0 soils were analyzed with a Carlo-Erba elemental analyzer (NC2500) at the German Research Center for Geosciences, Potsdam, Germany. The as-collected soils were oven dried at 40°C for 48 hours, sieved to <7 mm and crushed using a TEMA disk mill to achieve size fractions of < 20 µm. Total organic carbon (TOC) was analyzed after reacting the powders with a 10% HCl solution for 12 hours to remove inorganic carbonates.

2.3. Determination of maximum growth rates

The microbial activity was determined in 113 year old soil samples after they were thawed (in the dark at 5°C to mimic typical field temperature) for 168 hours. This age was chosen because these soil samples were assumed to be the ones with the highest microbial biomass and activity and thus the most appropriate for all laboratory measurements. Aliquots of the soils were divided into petri dishes (25 g of soil (wet weight) into each petri dish) for subsequent treatments. In order to alleviate nutrient limitations and measure maximum growth rates, four different nutrient conditions were simulated: (1) no addition of nutrients, (2) low (0.03 mg C g^{-1}, 0.008 mg N g^{-1}, 0.02 mg P g^{-1}), (3) medium (0.8 mg C g^{-1}, 0.015 mg N g^{-1}, 0.1 mg P g^{-1}) and (4) high additions (2.4 mg C g^{-1}, 0.024 mg N g^{-1}, 0.3 mg P g^{-1}). The ranges and concentrations were informed by similar experiments in recently exposed proglacial soils at the Damma Glacier, Switzerland (Goransson et al., 2011). Nutrients ($C_6H_{12}O_6$ for C, NH_4NO_3 for N and KH_2PO_4 for P) (Sigma, quality ≥99.0%) were dissolved in 2 mL Milli-Q water (0.2 µm

Biogeosciences Discuss., doi:10.5194/bg-2016-52, 2016
Manuscript under review for journal Biogeosciences
Published: 16 February 2016

filtered), and mixed into the soils using an ethanol-sterilized spatula. Samples were incubated at 25°C (for later comparison of growth rates with previous estimates (Frey et al., 2010)) in the dark for a further 72 hours with the lids on. Throughout the whole incubation time, at 24 hour intervals, additional 2 mL aliquots of Milli-Q water (0.2 µm filtered) were added to maintain approximate soil moisture conditions in each sample.

In these samples bacterial production was estimated by the incorporation of ^{3}H-leucine using the microcentrifuge method detailed in Kirchman (2001). After the initial 72 hour incubation period quadruplicate sample aliquots from the petri dish incubations and two trichloroacetic acid (TCA) killed control samples were incubated for 3 hours at 25°C for every nutrient treatment. Approximately 50 mg of soil was transferred to sterile micro-centrifuge tubes (2.0 mL, Fischer Scientific). Milli-Q (0.2 µm pre-filtered) water and ^{3}H-leucine was added to a final concentration of 100 nM (optimum leucine concentration was pre-determined by a saturation experiment, Fig. S1, Supplementary Information). The incubation was terminated by the addition of TCA to each tube. Tubes were then centrifuged at 15,000 g for 15 minutes, the supernatant was aspirated with a sterile pipette and removed, and 1 ml ice-cold 5% TCA was added to each tube. Tubes were then centrifuged again at 15,000g for 5 minutes, before again aspirating and removing the supernatant. 1mL ice-cold 80% ethanol was added and tubes were centrifuged at 15,000 g for 5 minutes, before the supernatant was aspirated and removed again and tubes were left to air dry for 12 hours. Finally, 1 mL of scintillation cocktail was added, samples were vortexed, and then counted by liquid scintillation (Perkin Elmer Liquid Scintillation Analyzer, Tri-Carb 2810 TR). Radioisotope activity of TCA-killed control samples was always less than 1.1% of the measured activity in live samples. There was a positive correlation between the amount of sediment added to the tubes and background counts representing disintegrations per minute (DPM). Counts were individually normalized by the amount of sediments (corrected for dry weight) used in each sample to discount for background DPM. Leucine incorporation rates were converted into bacterial carbon production following the methodology of Simon and Azam (1989). Bacterial abundance was estimated from each treatment after the 72 hour incubation period by microscopy. Five samples from each petri dish were counted for each nutrient treatment with negative controls yielding no detectable cells. One-way ANOVA (with post-hoc Tukey HSD) statistical tests were used for evaluations of the variability from the multiple treatments.

2.4. Temperature response

Microbial community respiration was determined by measuring CO_2 gas exchange rates in airtight incubation vials. Soil samples from the 113 year old site were defrosted and divided (25 g wet weight) in petri dishes as above, and 2 mL of Milli-Q water (0.2 µm filtered) was added (to maintain consistency of soil moisture with determination of bacterial production above). Samples were incubated at 5°C (T_1) and 25°C (T_2) in the dark for a further 72 hours. 2mL of 0.2 µm pre-filtered Milli-Q water was added to the T_1 sample (3 mL for T_2) at 24, 48 and 72 hours to maintain approximate soil moisture content. Two separate killed control tests (one furnaced at 450°C for 4 hours, and one autoclaved (3 cycles at 121°C)) were incubated at T_1 and T_2. Quintuple live and killed samples

Biogeosciences Discuss., doi:10.5194/bg-2016-52, 2016
Manuscript under review for journal Biogeosciences
Published: 16 February 2016

(roughly 1 g) were transferred into cleaned 20 mL glass vials (rinsed in 2% Decon, submersed in 10% HCl for 24 hours, rinsed 3 times with Milli-Q water and furnaced at 450°C for 4 hours). These were sealed (9°C, atmospheric pressure, ambient CO_2 of 405 ppm) with pre-sterilized Bellco butyl stoppers (pre-sterilized by boiling for 4 hours in 1M sodium hydroxide) and crimped shut with aluminum caps. Sealed vials were then incubated at T_1 and T_2 for 24 hours in darkness. After 24 hours, the headspace gas was removed with a gas-tight syringe and immediately analyzed on an EGM4 gas analyzer (PP Systems, calibrated using gas standards matching the expected range, precision 1.9%, 2*SE). Empty pre-sterilized vials were also incubated and analyzed. Following gas analysis, vials were opened and dried to a constant weight at 105°C to estimate moisture content and thus dry soil weight of these aliquots. Headspace CO_2 change (ppm) was converted to microbial respiration using the ideal gas law (n=PV/RT), assuming negligible changes in soil pore water pH (and therefore CO_2 solubility) during the incubation. CO_2 headspace changes resulting from killed controls and blanks were < 70% of the changes resulting from the incubations at T_1, and <7% of the changes observed at T_2. One-way ANOVA (with post-hoc Tukey HSD statistical tests) were used for comparison of multiple treatments. No significant differences in CO_2 headspace change between killed controls at T_1 and T_2 were detected ($P>0.05$).

2.5. Microbial Model: SHIMMER

SHIMMER (Bradley et al., 2015) mechanistically describes and predicts transformations in carbon, nitrogen and phosphorus through aggregated components of the microbial community as a system of interlinked ordinary differential equations. The model is 0-D and represents the soil as a homogeneous mix. Thus, light, temperature, nutrients, organic compounds and microbial biomass are assumed to be evenly distributed. It categorizes microbes into autotrophs (A_{1-3}) and heterotrophs (H_{1-3}), and further subdivides these based on 3 specific functional traits. Microbes derived from underneath the glacier (referred to as “subglacial microbes”) are termed A_1 and H_1. A_1 are chemolithoautotrophic, obtaining energy from the oxidation and reduction of inorganic compounds and carbon from the fixation of carbon dioxide. In contrast, H_1 rely on the breakdown of organic molecules for energy to support growth. A_2 and H_2 represent autotrophic and heterotrophic microbes commonly found in glacier forefield soils with no “special” characteristics, and will be referred to as “soil microbes”. A_3 and H_3 are autotrophs and heterotrophs that are able to fix atmospheric N_2 gas as a source of nitrogen in cases when dissolved inorganic nitrogen (DIN) stocks become limiting. Available organic substrate is assumed to be derived naturally from dead organic matter and allochthonous inputs. Labile compounds are immediately available fresh and highly reactive material, rapidly turned over by the microorganisms (S_1, ON_1, OP_1). Refractory compounds are less bioavailable and represents the bulk of substrate present in the non-living organic component of soil (S_2, ON_2, OP_2).

Microbial biomass responds dynamically to changing substrate and nutrient availability (expressed as Monod-kinetics), as well as changing environmental conditions (such as temperature and light). A Q_{10} temperature response function (T_f) is affixed to all metabolic processes including growth rates and

Biogeosciences Discuss., doi:10.5194/bg-2016-52, 2016
Manuscript under review for journal Biogeosciences
Published: 16 February 2016

death rates (Bradley et al., 2015), thus effectively slowing down or speeding up all life processes as temperature changes (Soetaert and Herman, 2009; Yoshitake et al., 2010; Schipper et al., 2014). Light limitation is expressed as Monod kinetics.

The following external forcings drive and regulate the system's dynamics:

- Photosynthetically-active radiation (PAR) (wavelength of approximately 400 to 700 nm) (W m^{-2}).
- Snow depth (m).
- Soil temperature (°C).
- Allochthonous inputs (µg g^{-1} day^{-1}).

Soil temperature (at 1 cm depth) for the entire of 2013 is provided by Alfred Wegener Institute for Polar and Marine Research (AWI) from the permafrost observatory near Ny-Ålesund, Svalbard. Similarly, PAR for 2013 are measured at the AWI surface radiation station near Ny-Ålesund, Svalbard. Averaged daily snow depth for 2009 to 2013 is provided by the Norwegian Meteorological Institute (eKlima). Allochthonous nutrient fluxes (inputs and leaching) are estimated based on an evaluation of nutrient budgets of the Midtre Lovénbreen catchment (Hodson et al., 2005) in which budgets for nutrient deposition rates and runoff concentrations are measured over two full summer-winter seasons and residual retention rates (excess of inputs) or depletion rates (excess of outputs) are inferred.

Initial conditions were informed by analysis of 0-years-of-exposure soil collected adjacent to the ice snout, and initial values for all state variables are presented in Table 1. Initial microbial biomass was estimated by microscopy as described above. Initial community structure was derived by 16S analysis of year-0 soils. An initial value for carbon substrate (S1 + S2) was estimated based on the average TOC content of year-0 soil. Bioavailability of model TOC was assumed to be 30% labile (S_1) and 70% refractory (S_2) (for consistency with Bradley et al. (2015)). Organic nitrogen (ON) and organic phosphorus (OP) were assumed to be stoichiometrically linked by the measured C:N:P ratio from the Damma Glacier forefield (from which the model was initially developed and tested (Bradley et al., 2015)). An initial value for DIN was taken from a previous evaluation of Svalbard tundra nitrogen dynamics, whereby the lowest value is taken to represent the soil of least development, according to traditional understanding of glacier forefields (Alves et al., 2013; Bradley et al., 2014). An initial value for dissolved inorganic phosphorous (DIP) was established stoichiometrically from previous model development and testing.

Model implementation and set-up is described in more detail in the Supplementary Information.

2.6. Model parameters

Maximum heterotrophic growth rate I_{maxH} (day^{-1}) was estimated by scaling the measured rate of bacterial production (µg C g^{-1} day^{-1}) (converted to dry weight) with total heterotrophic biomass (µg C g^{-}

Biogeosciences Discuss., doi:10.5194/bg-2016-52, 2016
Manuscript under review for journal Biogeosciences
Published: 16 February 2016

320 ^{1}). Nutrient addition alleviates growth limitations as defined in SHIMMER (Bradley, 2015); thus
321 bacterial communities can be assumed to be growing at I_{maxH} under experimental conditions.
322
323 Y_H represents heterotrophic BGE, and was estimated according to the equation:
324
325 $$Y_H = \frac{BP}{BP + BR} \quad (1)$$
326
327 Where *BP* is and *BR* are measured bacterial production and measured bacterial respiration (µg C g^{-1}
328 day^{-1}) respectively, at 25°C with no nutrients added.
329
330 The temperature response (Q_{10}) value was estimated as:
331
332 $$Q_{10} = \left(\frac{R_2}{R_1}\right)^{\left(\frac{10}{T_2 - T_1}\right)} \quad (2)$$
333
334 Where R_1 and R_2 represent the measured respiration rate (µg C g^{-1} day^{-1}) at temperatures T_1 and T_2
335 (5°C and 25°C).
336
337 Laboratory-defined parameters (i.e. growth rate, temperature sensitivity and BGE) were assumed to
338 be the same for all microbial groups. A complete list of parameters and values is presented in Table
339 S3 (Supplementary Information).
340
341 **3. Results**
342 **3.1. Laboratory results and model parameters**
343 Bacterial production in untreated soil was estimated at 0.76 µg C g^{-1} day^{-1}, and across all nutrient
344 treatments ranged from 0.560 to 2.196 µg C g^{-1} day^{-1}. Nutrient addition led to increased measured
345 production (low = 0.69 µg C g^{-1} day^{-1}, medium = 1.09 µg C g^{-1} day^{-1}, high = 1.52 µg C g^{-1} day^{-1}),
346 however variability between replicates was also high and production rates from each nutrient
347 treatment were not significantly different from untreated soil ($P > 0.05$). The increased bacterial
348 production was cross-correlated with quadruplicate measurements of biomass from each treatment,
349 and resulting growth rates for all treatments were within a narrow range (0.359 to 0.550 day^{-1}) and
350 there was no statistically significant difference in growth rates between each nutrient treatment (Fig.
351 2b) ($P < 0.05$). The maximum measured growth rate for a single nutrient treatment, thus equating to
352 the parameter I_{maxH}, was 0.55 day^{-1}. The 95% confidence range for I_{maxH} is 0.50 to 0.60 day^{-1}. For
353 respiration, significantly higher CO_2 headspace concentration were detected in the live incubations at
354 25˚C relative to killed controls ($P < 0.05$). Average respiration rate at 5°C was 1.61 C g^{-1} day^{-1} and
355 there was a significant increase in soil respiration at 25°C (12.83 µg C g^{-1} day^{-1}) (Fig. 2c) ($P < 0.05$).
356 The Q_{10} value for Midtre Lovénbreen forefield soils was thus calculated as 2.90, and a 95%
357 confidence range was established as 2.65 to 3.16. Based on measured values of bacterial production

Biogeosciences Discuss., doi:10.5194/bg-2016-52, 2016
Manuscript under review for journal Biogeosciences
Published: 16 February 2016

and respiration, BGE (Y_H) was 0.06, with a 95% confidence range of 0.05 to 0.07. Final calculated values for model parameters are summarized in Table S3 (Supplementary Information).

The results from microscopy determination of biomass are presented in Table 2. In the freshly exposed soil (year 0) heterotrophic biomass was low (0.059 µg C g^{-1}), increased substantially to 0.244 µg C g^{-1} in 29 year old soils, and was an order or magnitude higher (2.00 µg C g^{-1}) in 113 year old soils. Autotrophic biomass was considerably higher than heterotrophic biomass and increased by roughly an order of magnitude from year 0 (0.171 µg C g^{-1}) to year 29 (1.07 µg C g^{-1}) and approximately doubled by year 113 (2.58 µg C g^{-1}). TOC in freshly exposed soil was approximately 0.793 mg C g^{-1}).

16S data was categorized into microbial groups (A_{1-3} and H_{1-3}) as defined by the model formulation. Chemolitotrophs, such as known iron or sulfur oxidizers (genera *Acidothiobacillus*, *Thiobacillus*, *Gallionella*, *Sulfurimonas*) were assigned into the A_1 group. Phototrophic microorganisms, such as cyanobacteria (*Phormidium*, *Leptolyngbya*) and phototrophic bacteria (*Rhodoferax*, *Erythrobacter*, *Halomicronema*) were allocated into group A_2, while heterocyst forming, cyanobacteria from the orders Nostocales and Stigonematales were assigned to group the A_3 (nitrogen-fixing autotrophs). Members of the family Comamonadaceae of the Betaproteobacteria are known subglacial dwelling microorganisms (Yde et al., 2010) and were thus included into the group H_1. General soil heterotrophic microorganisms (mainly members of Alphaproteobacteria, Actinobacteria, Bacterioidetes and Acidobacteria) were assigned into group H_2 (general soil heterotrophs). Lastly, group H_3 consisted of heterotrophic nitrogen fixers, mainly *Azospirillum*, *Bradyrhizobium*, *Devosia*, *Clostridium*, *Frankia* and *Rhizobium*. Pathogens, non-soil microorganisms and organisms with unknown physiological traits were assigned into “Uncategorized” group. Subglacial microbes accounted for 43 to 45 % of reads in year 0 and 5, and declined in older soils (year 50 and 113) to 18 to 22%. The subglacial community was predominantly chemolithoautotrophic (A_1). Typical soil bacteria (A_2 and H_2) increased from low abundance (30% and 40% in years 0 and 5 respectively) to relatively high abundance (63 to 67%) of reads in years 50 and 113. Nitrogen fixing bacteria were prevalent in recently exposed soils (14% in year 0) but low in relative abundance in soils above 5 years of age (4 to 6% in years 5, 50 and 113). In the freshly exposed soil (year 0), the microbial community was relatively evenly distributed between heterotrophs (43%) and autotrophs (44%). In developed soils, the relative abundance of heterotrophs increased (up to 74% of reads in years 50 and 113). Important to note is the fact that between 8 and 21% of the reads across all samples could not be classified.

3.2. Model Results

The model predicted an accumulation of autotrophic and heterotrophic biomass over 120 years (Fig. 3a and 3b). Biomass and nutrient concentrations were initially extremely low (total biomass < 0.25 µg C g^{-1}, DIN < 4.0 µg N g^{-1}, DIP < 3.0 µg P g^{-1}), and biological activity in initial soils was also low (Table 3). There was an order of magnitude increase in total microbial biomass in years 10 to 60. Nitrogen-

Biogeosciences Discuss., doi:10.5194/bg-2016-52, 2016
Manuscript under review for journal Biogeosciences
Published: 16 February 2016

fixing autotrophs (A_3) and heterotrophs (H_3), and soil heterotrophs (H_2) experienced rapid growth during this period. Subglacial and soil autotrophs ($A_{1\text{-}2}$) and subglacial heterotrophs (H_1) remained low. Bacterial production increased by roughly two orders of magnitude (Table 3). Organic carbon (labile and refractory) increased (Fig. 3c), whilst DIN and DIP concentrations increased by approximately an order of magnitude in the first 60 years (Fig. 3d). During the later stages of soil development (years 60 to 120), biomass increased rapidly due to the rapid growth of soil organisms (A_2 and H_2), which outcompeted nitrogen-fixers. The model showed a rapid exhaustion of labile organic carbon (years 50 to 100), while refractory carbon accumulated slowly. Nutrients (DIN and DIP) accumulated at a relatively constant rate. Microbial activity, including bacterial production, nitrogen fixation and DIN assimilation, was high relative to early stages (Table 3).

A carbon budget of fluxes through the substrate pool is presented in Fig. 4. Daily fluxes are presented in panels (a) for year 5, (b) for year 50 and (c) for year 113, and annual fluxes up to year 120 are presented in (d). In recently exposed soils (5 years), allochthonous inputs were the only noticeable carbon flux, outweighing heterotrophic growth and respiration, and the contribution of substrate from necromass and exudates by over two orders of magnitude (Fig. 4a). Thus, the total change in carbon (black line) closely resembled allochthonous input. In the intermediate stages (Fig. 4b), there was substantial depletion from the substrate pool due to heterotrophic activity. Heterotrophic growth (red line) was low despite high substrate consumption and respiration (orange line). In the late stages of soil development, the flux of microbial necromass was a significant contributor to the organic substrate pools (Fig. 4c). Carbon fluxes in mid to late stages of soil development were highly seasonal (Fig. 4b and 4c). Biotic fluxes (e.g. respiration) were up to six times higher during the summer (July to September) compared to the winter (November to April), however a base rate of heterotrophic respiration and turnover of microbial biomass was sustained over winter. Figure 4d shows that the contribution of microbial necromass rose steadily throughout the simulation (blue line), however was not sufficient to compensate the uptake of carbon substrate, thus leading to overall depletion between years 50 to 110 (black line). The contribution of exudates (green line) to substrate was minimal at all soil ages.

4. Discussion

4.1. Determination of parameters and model predictions

The maximum microbial growth rate (I_{max}) was determined by incorporation of ^{3}H-leucine as 0.550 day^{-1}. This value is, to our knowledge, is the first measured rate of bacterial growth from High-Arctic soils, and falls within the lower end of the plausible range established in Bradley et al. (2015) (0.24 – 4.80 day^{-1}) for soil microbes from a range of laboratory and modelling studies (Fig. 5a) (Frey et al., 2010; Ingwersen et al., 2008; Knapp et al., 1983; Zelenev et al., 2000; Stapleton et al., 2005; Darrah, 1991; Blagodatsky et al., 1998; Vandewerf and Verstraete, 1987; Foereid and Yearsley, 2004; Toal et al., 2000; Scott et al., 1995). Figure 6 illustrates the influence of the site-specific, laboratory-derived parameters on microbial biomass predictions. It compares the range of predicted microbial biomass based on laboratory-determined parameters (yellow) to the entire plausible parameter range (red;

Biogeosciences Discuss., doi:10.5194/bg-2016-52, 2016
Manuscript under review for journal Biogeosciences
Published: 16 February 2016

438 Bradley et al. (2015)). Predicted biomass with the average laboratory-derived value is indicated by the
439 black line. For I_{max}, predicted biomass with laboratory-derived parameters (yellow shading) was
440 towards the lower end of the plausible range (Fig. 6a) because refined growth rates were significantly
441 lower than the maximum values explored previously. This was mostly due to a significant reduction in
442 autotrophic biomass ($A_{1\text{-}3}$). With high growth rates, there was a sharp early increase in biomass (years
443 10 to 20) followed by slower growth phase (years 20 to 120). Model results with laboratory-derived
444 growth rates showed that the exponential growth phase occurred later (years 40 to 80) and was more
445 prolonged, but total biomass was considerably lower. There was a substantial reduction in the
446 plausible range in predicted microbial biomass.
447
448 The laboratory-derived Q_{10} for Midtre Lovénbreen was at the upper end of the plausible range
449 previously identified in Bradley et al. (2015) (Fig. 5b). There was a substantial reduction in the
450 plausible range in predicted microbial biomass (Fig. 6b) from the measured temperature sensitivity
451 (yellow) compared to the previous range (red). Soil microbial communities in Polar regions must
452 contend with extremely harsh environmental conditions such as cold temperatures, frequent freeze-
453 thaw cycles, low water availability, low nutrient availability, high exposure to ultraviolet radiation in the
454 summer, and prolonged periods of darkness in winter. These factors profoundly impact their
455 metabolism and survival strategies and ultimately shape the structure of the microbial community
456 (Cary et al., 2010). High Q_{10} values, as derived here, are typical of cold environments and cold
457 adapted organisms and this has been associated with the survival of biomass under prolonged
458 periods of harsh environmental conditions (Schipper et al., 2014). An investigation into the
459 metabolism of microbial communities in biological soils crusts in recently exposed soils from the East
460 Brøgger Glacier, approximately 6 km from the Midtre Lovénbreen catchment, also derived a high Q_{10}
461 (3.1) (Yoshitake et al., 2010). The Midtre Lovénbreen catchment, in Svalbard, experiences a relatively
462 extreme Arctic climate. The high Q_{10} ultimately lowers the overall rate of biomass accumulation in
463 ultra-oligotrophic soils and a baseline population is maintained.
464
465 Measured BGE (Y_H) was 0.06 (Fig. 5c). The low BGE calculated here suggested that a high
466 proportion (94%) of substrate consumed by heterotrophs is recycled (degrading organic substrate into
467 DIC (CO_2), DIN and DIP), with very little being incorporated into biomass (6%). Low BGE encouraged
468 the liberation and release of nutrients to the soil and thus the overall growth response of the total
469 microbial biomass was more rapid due to higher soil nutrient concentrations (Fig. 6c). However, due
470 to the low BGE, there was a high rate of substrate degradation, and as such, labile substrate was
471 rapidly depleted when heterotrophic biomass was high (Fig. 3c). Heterotrophic growth requires that a
472 substantial amount of substrate is degraded – thus, although autotrophic production outweighed
473 heterotrophic production at all stages of development (Fig. 3e), the soil was predicted by the model to
474 be a net source of CO_2 to the atmosphere over the first 120 years of exposure (Fig. 3f). There are
475 very few measurements of BGE in cold glaciated environments, however previous studies have
476 suggested values as low as 0.0035 to 0.033 (Anesio et al., 2010; Hodson et al., 2007).
477

Biogeosciences Discuss., doi:10.5194/bg-2016-52, 2016
Manuscript under review for journal Biogeosciences
Published: 16 February 2016

478 **4.2. Microbial biomass dynamics and community structure**

479 Measured microbial biomass in the initial soils of Midtre Lovénbreen (0.23 µg C g^{-1}, 0 years) was very
480 low compared to initial soils in other deglaciated forefields of equivalent ages in lower latitudes, for
481 example in the Alps (4 µg C g^{-1}) (Bernasconi et al., 2011; Tscherko et al., 2003) and Canada (6 µg C
482 g^{-1}) (Insam and Haselwandter, 1989). However, our microbial biomass values are more similar to
483 other recently deglaciated soils in Antarctica (Ecology Glacier - 0.88 µg C g^{-1}) (Zdanowski et al.,
484 2013). Low biomass is possibly a result of the harsh, ultra-oligotrophic and nutrient limiting
485 environment of the High Arctic and Antarctica, where low temperature and longer winters limit the
486 summer growth phase, especially compared to an Alpine system (Tscherko et al., 2003; Bernasconi
487 et al., 2011).
488
489 The initial microbial community structure in our samples was predominantly autotrophic (74.5%). In
490 the years following exposure, we observed an increase in autotrophs and heterotrophs with soil age
491 (Table 3), presumably due to the establishment and growth of stable soil microbial communities
492 (Schulz et al., 2013; Bradley et al., 2014). Both the observations and modelling results suggested that
493 there was no substantial increase in heterotrophic biomass during the initial and early-intermediate
494 stages of soil development (years 0 to 40), which was then followed by a growth phase whereby
495 biomass increased by roughly an order of magnitude. Overall, the model and the microscopy data
496 were in good agreement accounting for the limitations in both techniques, spatial heterogeneity, and
497 the oscillations in biomass arising from seasonality. The pattern of microbial abundance observed in
498 the Midtre Lovénbreen forefield broadly resembles that of other glacier forefields worldwide (Insam
499 and Haselwandter, 1989; Bernasconi et al., 2011; Schulz et al., 2013).
500
501 The genomic data indicated that subglacial microbes are dominant in recently exposed soils, in
502 agreement with model results (Fig. 8). The community structure in year 5 was heavily dominated by
503 chemolithoautotrophs (A_1), which reflected findings from previous studies whereby
504 chemolithoautotrophic bacteria contribute to the oxidation of FeS_2 in proglacial moraines in Midtre
505 Lovénbreen (Borin et al., 2010; Mapelli et al., 2011). These processes are also commonly described
506 in other subglacial habitats (Boyd et al., 2014; Hamilton et al., 2013). Based on 16S data, the
507 subglacial community declined in relative abundance with soil age. This finding was also reflected in
508 the model in years 50 and 113. As the age of the soil progressed, there was typically greater
509 abundance of microbes representing typical soil bacteria (groups A_2 and H_2) in the 16S data and the
510 model, thus the relative abundance of subglacial microbes decreased. Microscopy and modelling
511 indicated a predominantly autotrophic community, however 16S data indicated the contrary –
512 especially in the later stages of soil development. Nevertheless, both the 16S and microscopy data
513 indicated that there was a mixed community of autotrophs and heterotrophs in soils of all ages, which
514 was supported by modelling, since no functional groups were extirpated over simulations representing
515 120 years of soil development.
516

Biogeosciences Discuss., doi:10.5194/bg-2016-52, 2016
Manuscript under review for journal Biogeosciences
Published: 16 February 2016

517 Nitrogen-fixing bacteria were prevalent in recently exposed soils but declined in relative abundance
518 with soil age. By fixing N_2 instead of assimilating DIN, the model predicted that nitrogen-fixers were
519 able to grow rapidly in the early stages relative to other organisms (Fig. 3a and 3b). The model
520 prediction supports findings by previous studies demonstrating the importance of nitrogen fixation in
521 glacier forefields (Duc et al., 2009; Schmidt et al., 2008; Strauss et al., 2012) and other glacial
522 ecosystems (Telling et al., 2011; Telling et al., 2012). However, there was poor agreement on the
523 relative abundance of nitrogen fixers between the model and the 16S data in the later stages of soil
524 development (years 50 to 120). The model over-predicted the relative abundance of nitrogen fixing
525 organisms (Fig. 8). The majority of the biomass of the autotrophic nitrogen fixers was composed of
526 sequences belonging to the cyanobacterium from the genus *Nostoc*. *Nostoc* forms macroscopically
527 visible colonies that grow on the surface of the soils. Its distribution in the Arctic soils is thus extremely
528 patchy and therefore part of the discrepancy between the 16S data and the model regarding the
529 relative distribution of the A_3 group in the older soils could be due to under-sampling of the *Nostoc*
530 colonies. Allochthonous inputs of nitrogen to the Arctic (e.g. aerial deposition (Geng et al., 2014))
531 strongly affect the productivity of microbial ecosystems and the requirement of nitrogen fixation for
532 microbes (Bjorkman et al., 2013; Kuhnel et al., 2013; Kuhnel et al., 2011; Hodson et al., 2010; Telling
533 et al., 2012; Galloway et al., 2008). Thus, uncertainty in the allochthonous availability of nitrogen
534 strongly affects nitrogen fixation rates. In attempting to replicate a qualitative understanding of the
535 nitrogen cycle in a quantitative mathematical modelling framework, the predicted importance of
536 nitrogen-fixing organisms may be over-estimated. The poor agreement in the relative abundance of
537 nitrogen-fixers between the model and the 16S data indicates an incomplete understanding of
538 allochthonous versus autochthonous nutrient availability. Allochthonous nutrient availability is a known
539 source of uncertainty (Bradley et al., 2014; Schulz et al., 2013; Schmidt et al., 2008), and addressing
540 this concern is the subject of future work.
541
542 **4.3. Net ecosystem metabolism and carbon budget**
543 The seasonality of carbon fluxes predicted by the model (Fig. 4b and 4c) related to the high measured
544 Q_{10} values. High seasonal variation in biotic fluxes and rates is typical of cryospheric soil ecosystems
545 (Schostag et al., 2015) including glacier forefield soils (Lazzaro et al., 2012; Lazzaro et al., 2015).
546 However, microbial activity has been shown to persist during winter under insulating layers of snow
547 and in sub-zero temperatures (Zhang et al., 2014). Modelling also predicted sustained organic
548 substrate degradation, microbial turnover and net heterotrophy during the winter (Fig. 4b and 4c), as
549 documented in other glacier forefield studies (Guelland et al., 2013b), at a low rate.
550
551 The low measured BGE has three important consequences. Firstly, low BGE suggests that a large
552 pool of substrate is required to support heterotrophic growth. Low-efficiency heterotrophic growth lead
553 to the rapid depletion of substrate; therefore high allochthonous inputs were required to maintain a
554 sizeable pool. In older soils (years 80 to 120), increased inputs from microbial necromass (blue line,
555 Fig. 4d) sustained substrate supply to heterotrophs. The sources of allochthonous carbon substrate to
556 the glacier forefield include meltwater inputs derived from the supraglacial and subglacial ecosystems

(Stibal et al., 2008; Hodson et al., 2005; Mindl et al., 2007), snow algae (which are known to be prolific primary colonizers and producers in High Arctic snow packs (Lutz et al., 2015; Lutz et al., 2014), atmospheric deposition (Kuhnel et al., 2013) and ornithogenic deposition (e.g. fecal matter of birds and animals) (Jakubas et al., 2008; Ziolek and Melke, 2014; Luoto et al., 2015; Michelutti et al., 2009; Michelutti et al., 2011; Moe et al., 2009). Microbial dynamics are moderately sensitive to external allochthonous inputs of substrate (Bradley et al., 2015), and addressing the uncertainty associated with this flux is an important question to address in future research.

Secondly, low BGE causes a net efflux of CO_2 over the first 120 years of soil development despite high autotrophic production (Fig. 3e and 3f). Recent literature has explored the carbon dynamics of glacier forefield ecosystems, finding highly variable soil respiration rates (Bekku et al., 2004; Schulz et al., 2013; Guelland et al., 2013a). Future studies should focus on quantifying carbon and nutrient transformations and the potential for forefield systems to impact global biogeochemical cycles in response to future climate change (Smittenberg et al., 2012) and in the context of large-scale ice retreat.

Thirdly, high rates of substrate degradation encouraged by low BGE were responsible for rapid nutrient release. Modelling suggested that microbial growth was strongly inhibited by low nutrient availability in initial soils (4 µg N g^{-1}, 2 to 10 µg P g^{-1}) (Fig. 3d). This is consistent with findings from the Hailuogou Glacier (Gongga Shan, China) and Damma Glacier (Switzerland) (Prietzel et al., 2013). Low BGE is predicted by the model to have a very important role in encouraging the release of nutrients from organic material more rapidly, thereby increasing total bacterial production in the intermediate stages of soil development. Increased nutrient availability with increased heterotrophic biomass is consistent with recent observations from glacier forefields (Bekku et al., 2004; Schulz et al., 2013; Schmidt et al., 2008).

5. Conclusions

We used laboratory-based mesocosm experiments to measure three key model parameters: maximum microbial growth rate (I_{max}) (by incorporation of ^{3}H-leucine), BGE (Y) (by measuring respiration rates) and the temperature response (Q_{10}) (by measuring rates at different ambient temperatures). Laboratory-derived parameters were comparable with previous estimations, and refined model predictions by narrowing the range of model output over nominal environmental conditions, thus increasing confidence in model predictions. Our results demonstrated that microbial dynamics at the initial stages of soil development in glacial forefields do not contribute to significant accumulation of organic carbon due the very low growth efficiency of the microbial community, resulting in a net efflux of CO_2 from those habitats. However, the low bacterial growth efficiency in glacial forefields is also responsible for high rates of nutrient recycling that most probably have an important role on the establishment of plants at older ages. The relative importance of allochthonous versus autochthonous substrate and nutrients is the focus of future research.

Much of the extreme ice-free regions in Antarctica are characterized by a complete absence of higher order plants. However even these environments contain diverse microbial populations and extremely low but detectable levels of organic carbon (Cowan et al., 2014), making these environments suitable cases for modelling using SHIMMER. This exercise shows how an integrated model-data approach can improve understanding and predictions of microbial dynamics in forefield soils and disentangle complex processes interactions to ascertain the relative importance of each process independently. This combined approach explored detailed microbial and biogeochemical dynamics of soil development with the view to obtaining a more holistic picture of soil development in a warmer and increasingly ice-free future world.

Acknowledgements

We thank Siegrid Debatin, Marion Maturilli, and Julia Boike (AWI) for support in acquiring meteorological and radiation data, Simon Cobb and James Williams (University of Bristol) for laboratory assistance, and Nicholas Cox and James Wake for assistance in the field and use of the UK Station Arctic Research base in Ny-Ålesund. This research was supported by NERC grant no. NE/J02399X/1 to A. M. Anesio. S. Arndt acknowledges support from NERC grant no. NE/IO21322/1.

References

ACIA: Arctic Climate Impacts Assessment, Cambridge University Press, Cambridge, 1042, 2005.

Alves, R. J. E., Wanek, W., Zappe, A., Richter, A., Svenning, M. M., Schleper, C., and Urich, T.: Nitrification rates in Arctic soils are associated with functionally distinct populations of ammonia-oxidizing archaea, Isme J, 7, 1620-1631, 10.1038/ismej.2013.35, 2013.

Anderson, S. P., Drever, J. I., Frost, C. D., and Holden, P.: Chemical weathering in the foreland of a retreating glacier, Geochim Cosmochim Ac, 64, 1173-1189, Doi 10.1016/S0016-7037(99)00358-0, 2000.

Anesio, A. M., Hodson, A. J., Fritz, A., Psenner, R., and Sattler, B.: High microbial activity on glaciers: importance to the global carbon cycle, Global Change Biol, 15, 955-960, DOI 10.1111/j.1365-2486.2008.01758.x, 2009.

Anesio, A. M., Sattler, B., Foreman, C., Telling, J., Hodson, A., Tranter, M., and Psenner, R.: Carbon fluxes through bacterial communities on glacier surfaces, Ann Glaciol, 51, 32-40, 2010.

Bekku, Y. S., Nakatsubo, T., Kume, A., and Koizumi, H.: Soil microbial biomass, respiration rate, and temperature dependence on a successional glacier foreland in Ny-Alesund, Svalbard, Arct Antarct Alp Res, 36, 395-399, 2004.

Bernasconi, S. M., Bauder, A., Bourdon, B., Brunner, I., Bunemann, E., Christl, I., Derungs, N., Edwards, P., Farinotti, D., Frey, B., Frossard, E., Furrer, G., Gierga, M., Goransson, H., Gulland, K., Hagedorn, F., Hajdas, I., Hindshaw, R., Ivy-Ochs, S., Jansa, J., Jonas, T., Kiczka, M., Kretzschmar, R., Lemarchand, E., Luster, J., Magnusson, J., Mitchell, E. A. D., Venterink, H. O., Plotze, M., Reynolds, B., Smittenberg, R. H., Stahli, M., Tamburini, F., Tipper, E. T., Wacker, L., Welc, M., Wiederhold, J. G., Zeyer, J., Zimmermann, S., and Zumsteg, A.: Chemical and Biological Gradients along the Damma Glacier Soil Chronosequence, Switzerland, Vadose Zone J, 10, 867-883, Doi 10.2136/Vzj2010.0129, 2011.

641 Berner, R. A., Lasaga, A. C., and Garrels, R. M.: The Carbonate-Silicate Geochemical Cycle
642 and Its Effect on Atmospheric Carbon-Dioxide over the Past 100 Million Years, Am J Sci, 283,
643 641-683, 1983.
644 Billings, W. D.: Carbon Balance of Alaskan Tundra and Taiga Ecosystems - Past, Present and
645 Future, Quaternary Sci Rev, 6, 165-177, Doi 10.1016/S0277-3791(00)90007-6, 1987.
646 Bjorkman, M. P., Kuhnel, R., Partridge, D. G., Roberts, T. J., Aas, W., Mazzola, M., Viola, A.,
647 Hodson, A., Strom, J., and Isaksson, E.: Nitrate dry deposition in Svalbard, Tellus B, 65, Artn
648 19071
649 Doi 10.3402/Tellusb.V65i0.19071, 2013.
650 Blagodatsky, S. A., Yevdokimov, I. V., Larionova, A. A., and Richter, J.: Microbial growth in
651 soil and nitrogen turnover: Model calibration with laboratory data, Soil Biol Biochem, 30,
652 1757-1764, Doi 10.1016/S0038-0717(98)00029-7, 1998.
653 Borin, S., Ventura, S., Tambone, F., Mapelli, F., Schubotz, F., Brusetti, L., Scaglia, B., D'Acqui,
654 L. P., Solheim, B., Turicchia, S., Marasco, R., Hinrichs, K. U., Baldi, F., Adani, F., and
655 Daffonchio, D.: Rock weathering creates oases of life in a High Arctic desert, Environ
656 Microbiol, 12, 293-303, DOI 10.1111/j.1462-2920.2009.02059.x, 2010.
657 Boyd, E. S., Hamilton, T. L., Havig, J. R., Skidmore, M. L., and Shock, E. L.: Chemolithotrophic
658 Primary Production in a Subglacial Ecosystem, Appl Environ Microb, 80, 6146-6153,
659 10.1128/Aem.01956-14, 2014.
660 Bradley, J. A., Singarayer, J. S., and Anesio, A. M.: Microbial community dynamics in the
661 forefield of glaciers, Proceedings. Biological sciences / The Royal Society, 281, 2793-2802,
662 10.1098/rspb.2014.0882, 2014.
663 Bradley, J. A., Anesio, A. M., Singarayer, J. S., Heath, M. R., and Arndt, S.: SHIMMER (1.0): a
664 novel mathematical model for microbial and biogeochemical dynamics in glacier forefield
665 ecosystems, Geosci. Model Dev., 8, 3441-3470, 10.5194/gmd-8-3441-2015, 2015.
666 Bradley, J. A., Anesio, A., and Arndt, S.: Bridging the divide: a model-data approach to Polar
667 & Alpine Microbiology, Fems Microbiol Ecol, 10.1093/femsec/fiw015, 2016.
668 Bratbak, G., and Dundas, I.: Bacterial Dry-Matter Content and Biomass Estimations, Appl
669 Environ Microb, 48, 755-757, 1984.
670 Brown, S. P., and Jumpponen, A.: Contrasting primary successional trajectories of fungi and
671 bacteria in retreating glacier soils, Mol Ecol, 23, 481-497, Doi 10.1111/Mec.12487, 2014.
672 Caporaso, J. G., Kuczynski, J., Stombaugh, J., Bittinger, K., Bushman, F. D., Costello, E. K.,
673 Fierer, N., Pena, A. G., Goodrich, J. K., Gordon, J. I., Huttley, G. A., Kelley, S. T., Knights, D.,
674 Koenig, J. E., Ley, R. E., Lozupone, C. A., McDonald, D., Muegge, B. D., Pirrung, M., Reeder, J.,
675 Sevinsky, J. R., Tumbaugh, P. J., Walters, W. A., Widmann, J., Yatsunenko, T., Zaneveld, J.,
676 and Knight, R.: QIIME allows analysis of high-throughput community sequencing data, Nat
677 Methods, 7, 335-336, 10.1038/nmeth.f.303, 2010.
678 Cary, S. C., McDonald, I. R., Barrett, J. E., and Cowan, D. A.: On the rocks: the microbiology of
679 Antarctic Dry Valley soils, Nat Rev Microbiol, 8, 129-138, 10.1038/nrmicro2281, 2010.
680 Cowan, D. A., Makhalanyane, T. P., Dennis, P. G., and Hopkins, D. W.: Microbial ecology and
681 biogeochemistry of continental Antarctic soils, Frontiers in microbiology, 5, Artn 154
682 Doi 10.3389/Fmicb.2014.00154, 2014.
683 Darrah, P. R.: Models of the Rhizosphere .1. Microbial-Population Dynamics around a Root
684 Releasing Soluble and Insoluble Carbon, Plant Soil, 133, 187-199, Doi 10.1007/Bf00009191,
685 1991.

686 Dessert, C., Dupre, B., Gaillardet, J., Francois, L. M., and Allegre, C. J.: Basalt weathering laws
687 and the impact of basalt weathering on the global carbon cycle, Chem Geol, 202, 257-273,
688 DOI 10.1016/j.chemgeo.2002.10.001, 2003.
689 Duc, L., Noll, M., Meier, B. E., Burgmann, H., and Zeyer, J.: High Diversity of Diazotrophs in
690 the Forefield of a Receding Alpine Glacier, Microbial Ecol, 57, 179-190, DOI 10.1007/s00248-
691 008-9408-5, 2009.
692 Dyurgerov, M. B., and Meier, M. F.: Twentieth century climate change: Evidence from small
693 glaciers, P Natl Acad Sci USA, 97, 1406-1411, DOI 10.1073/pnas.97.4.1406, 2000.
694 Edgar, R. C., Haas, B. J., Clemente, J. C., Quince, C., and Knight, R.: UCHIME improves
695 sensitivity and speed of chimera detection, Bioinformatics, 27, 2194-2200,
696 10.1093/bioinformatics/btr381, 2011.
697 Ensign, K. L., Webb, E. A., and Longstaffe, F. J.: Microenvironmental and seasonal variations
698 in soil water content of the unsaturated zone of a sand dune system at Pinery Provincial
699 Park, Ontario, Canada, Geoderma, 136, 788-802, DOI 10.1016/j.geoderma.2006.06.009,
700 2006.
701 Esperschutz, J., Perez-de-Mora, A., Schreiner, K., Welzl, G., Buegger, F., Zeyer, J., Hagedorn,
702 F., Munch, J. C., and Schloter, M.: Microbial food web dynamics along a soil chronosequence
703 of a glacier forefield, Biogeosciences, 8, 3283-3294, DOI 10.5194/bg-8-3283-2011, 2011.
704 Filippelli, G. M.: The global phosphorus cycle, Rev Mineral Geochem, 48, 391-425, DOI
705 10.2138/rmg.2002.48.10, 2002.
706 Fleming, K. M., Dowdeswell, J. A., and Oerlemans, J.: Modelling the mass balance of
707 northwest Spitsbergen glaciers and responses to climate change, Annals of Glaciology, Vol
708 24, 1997, 24, 203-210, 1997.
709 Foereid, B., and Yearsley, J. M.: Modelling the impact of microbial grazers on soluble
710 rhizodeposit turnover, Plant Soil, 267, 329-342, DOI 10.1007/s11104-005-0139-9, 2004.
711 Follmi, K. B., Hosein, R., Arn, K., and Steinmann, P.: Weathering and the mobility of
712 phosphorus in the catchments and forefields of the Rhone and Oberaar glaciers, central
713 Switzerland: Implications for the global phosphorus cycle on glacial-interglacial timescales,
714 Geochim Cosmochim Ac, 73, 2252-2282, DOI 10.1016/j.gca.2009.01.017, 2009.
715 Fountain, A. G., Nylen, T. H., Tranter, M., and Bagshaw, E.: Temporal variations in physical
716 and chemical features of cryoconite holes on Canada Glacier, McMurdo Dry Valleys,
717 Antarctica, J Geophys Res-Biogeo, 113, Artn G01s92
718 Doi 10.1029/2007jg000430, 2008.
719 Frey, B., Rieder, S. R., Brunner, I., Plotze, M., Koetzsch, S., Lapanje, A., Brandl, H., and Furrer,
720 G.: Weathering-Associated Bacteria from the Damma Glacier Forefield: Physiological
721 Capabilities and Impact on Granite Dissolution, Appl Environ Microb, 76, 4788-4796, Doi
722 10.1128/Aem.00657-10, 2010.
723 Frey, B., Buhler, L., Schmutz, S., Zumsteg, A., and Furrer, G.: Molecular characterization of
724 phototrophic microorganisms in the forefield of a receding glacier in the Swiss Alps, Environ
725 Res Lett, 8, Artn 015033
726 Doi 10.1088/1748-9326/8/1/015033, 2013.
727 Galloway, J. N., Townsend, A. R., Erisman, J. W., Bekunda, M., Cai, Z. C., Freney, J. R.,
728 Martinelli, L. A., Seitzinger, S. P., and Sutton, M. A.: Transformation of the nitrogen cycle:
729 Recent trends, questions, and potential solutions, Science, 320, 889-892,
730 10.1126/science.1136674, 2008.

731 Geng, L., Alexander, B., Cole-Dai, J., Steig, E. J., Savarino, J., Sofen, E. D., and Schauer, A. J.:
732 Nitrogen isotopes in ice core nitrate linked to anthropogenic atmospheric acidity change, P
733 Natl Acad Sci USA, 111, 5808-5812, 10.1073/pnas.1319441111, 2014.
734 Goransson, H., Venterink, H. O., and Baath, E.: Soil bacterial growth and nutrient limitation
735 along a chronosequence from a glacier forefield, Soil Biol Biochem, 43, 1333-1340, DOI
736 10.1016/j.soilbio.2011.03.006, 2011.
737 Goulden, M. L., Wofsy, S. C., Harden, J. W., Trumbore, S. E., Crill, P. M., Gower, S. T., Fries, T.,
738 Daube, B. C., Fan, S. M., Sutton, D. J., Bazzaz, A., and Munger, J. W.: Sensitivity of boreal
739 forest carbon balance to soil thaw, Science, 279, 214-217, DOI
740 10.1126/science.279.5348.214, 1998.
741 Guelland, K., Esperschutz, J., Bornhauser, D., Bernasconi, S. M., Kretzschmar, R., and
742 Hagedorn, F.: Mineralisation and leaching of C from C-13 labelled plant litter along an initial
743 soil chronosequence of a glacier forefield, Soil Biol Biochem, 57, 237-247, DOI
744 10.1016/j.soilbio.2012.07.002, 2013a.
745 Guelland, K., Hagedorn, F., Smittenberg, R. H., Goransson, H., Bernasconi, S. M., Hajdas, I.,
746 and Kretzschmar, R.: Evolution of carbon fluxes during initial soil formation along the
747 forefield of Damma glacier, Switzerland, Biogeochemistry, 113, 545-561, DOI
748 10.1007/s10533-012-9785-1, 2013b.
749 Hamilton, T. L., Peters, J. W., Skidmore, M. L., and Boyd, E. S.: Molecular evidence for an
750 active endogenous microbiome beneath glacial ice, Isme J, 7, 1402-1412,
751 10.1038/ismej.2013.31, 2013.
752 Hodkinson, I. D., Coulson, S. J., and Webb, N. R.: Community assembly along proglacial
753 chronosequences in the high Arctic: vegetation and soil development in north-west
754 Svalbard, J Ecol, 91, 651-663, DOI 10.1046/j.1365-2745.2003.00786.x, 2003.
755 Hodson, A., Anesio, A. M., Ng, F., Watson, R., Quirk, J., Irvine-Fynn, T., Dye, A., Clark, C.,
756 McCloy, P., Kohler, J., and Sattler, B.: A glacier respires: Quantifying the distribution and
757 respiration CO2 flux of cryoconite across an entire Arctic supraglacial ecosystem, J Geophys
758 Res-Biogeo, 112, Artn G04s36
759 Doi 10.1029/2007jg000452, 2007.
760 Hodson, A., Roberts, T. J., Engvall, A. C., Holmen, K., and Mumford, P.: Glacier ecosystem
761 response to episodic nitrogen enrichment in Svalbard, European High Arctic,
762 Biogeochemistry, 98, 171-184, DOI 10.1007/s10533-009-9384-y, 2010.
763 Hodson, A. J., Mumford, P. N., Kohler, J., and Wynn, P. M.: The High Arctic glacial ecosystem:
764 new insights from nutrient budgets, Biogeochemistry, 72, 233-256, DOI 10.1007/s10533-
765 004-0362-0, 2005.
766 Ingwersen, J., Poll, C., Streck, T., and Kandeler, E.: Micro-scale modelling of carbon turnover
767 driven by microbial succession at a biogeochemical interface, Soil Biol Biochem, 40, 864-878,
768 DOI 10.1016/j.soilbio.2007.10.018, 2008.
769 Insam, H., and Haselwandter, K.: Metabolic Quotient of the Soil Microflora in Relation to
770 Plant Succession, Oecologia, 79, 174-178, Doi 10.1007/Bf00388474, 1989.
771 Jakubas, D., Zmudczynska, K., Wojczulanis-Jakubas, K., and Stempniewicz, L.: Faeces
772 deposition and numbers of vertebrate herbivores in the vicinity of planktivorous and
773 piscivorous seabird colonies in Hornsund, Spitsbergen, Pol Polar Res, 29, 45-58, 2008.
774 Johannessen, O. M., Bengtsson, L., Miles, M. W., Kuzmina, S. I., Semenov, V. A., Alekseev, G.
775 V., Nagurnyi, A. P., Zakharov, V. F., Bobylev, L. P., Pettersson, L. H., Hasselmann, K., and
776 Cattle, A. P.: Arctic climate change: observed and modelled temperature and sea-ice
777 variability, Tellus A, 56, 328-341, DOI 10.1111/j.1600-0870.2004.00060.x, 2004.

778 Kastovska, K., Elster, J., Stibal, M., and Santruckova, H.: Microbial assemblages in soil
779 microbial succession after glacial retreat in Svalbard (high Arctic), Microbial Ecol, 50, 396-
780 407, DOI 10.1007/s00248-005-0246-4, 2005.
781 King, A. J., Meyer, A. F., and Schmidt, S. K.: High levels of microbial biomass and activity in
782 unvegetated tropical and temperate alpine soils, Soil Biol Biochem, 40, 2605-2610, DOI
783 10.1016/j.soilbio.2008.06.026, 2008.
784 Kirchman, D.: Measuring Bacterial Biomass Production and Growth Rates from Leucine
785 Incorporation in Natural Aquatic Environments in: Marine Microbiology, edited by: Paul, J.
786 H., Academic Press, London, UK, 2001.
787 Kirschke, S., Bousquet, P., Ciais, P., Saunois, M., Canadell, J. G., Dlugokencky, E. J.,
788 Bergamaschi, P., Bergmann, D., Blake, D. R., Bruhwiler, L., Cameron-Smith, P., Castaldi, S.,
789 Chevallier, F., Feng, L., Fraser, A., Heimann, M., Hodson, E. L., Houweling, S., Josse, B.,
790 Fraser, P. J., Krummel, P. B., Lamarque, J. F., Langenfelds, R. L., Le Quere, C., Naik, V.,
791 O'Doherty, S., Palmer, P. I., Pison, I., Plummer, D., Poulter, B., Prinn, R. G., Rigby, M.,
792 Ringeval, B., Santini, M., Schmidt, M., Shindell, D. T., Simpson, I. J., Spahni, R., Steele, L. P.,
793 Strode, S. A., Sudo, K., Szopa, S., van der Werf, G. R., Voulgarakis, A., van Weele, M., Weiss,
794 R. F., Williams, J. E., and Zeng, G.: Three decades of global methane sources and sinks, Nat
795 Geosci, 6, 813-823, Doi 10.1038/Ngeo1955, 2013.
796 Knapp, E. B., Elliott, L. F., and Campbell, G. S.: Carbon, Nitrogen and Microbial Biomass
797 Interrelationships during the Decomposition of Wheat Straw - a Mechanistic Simulation-
798 Model, Soil Biol Biochem, 15, 455-461, Doi 10.1016/0038-0717(83)90011-1, 1983.
799 Kuhnel, R., Roberts, T. J., Bjorkman, M. P., Isaksson, E., Aas, W., Holmen, K., and Strom, J.:
800 20-Year Climatology of NO3- and NH4+ Wet Deposition at Ny-Alesund, Svalbard, Adv
801 Meteorol, Artn 406508
802 Doi 10.1155/2011/406508, 2011.
803 Kuhnel, R., Bjorkman, M. P., Vega, C. P., Hodson, A., Isaksson, E., and Strom, J.: Reactive
804 nitrogen and sulphate wet deposition at Zeppelin Station, Ny-Alesund, Svalbard, Polar Res,
805 32, Unsp 19136
806 Doi 10.3402/Polar.V32i0.19136, 2013.
807 Lazzaro, A., Brankatschk, R., and Zeyer, J.: Seasonal dynamics of nutrients and bacterial
808 communities in unvegetated alpine glacier forefields, Appl Soil Ecol, 53, 10-22, DOI
809 10.1016/j.apsoil.2011.10.013, 2012.
810 Lazzaro, A., Hilfiker, D., and Zeyer, J.: Structures of Microbial Communities in Alpine Soils:
811 Seasonal and Elevational Effects, Frontiers in microbiology, 6, ARTN 1330
812 10.3389/fmicb.2015.01330, 2015.
813 Lee, S.: A theory for polar amplification from a general circulation perspective, Asia-Pac J
814 Atmos Sci, 50, 31-43, DOI 10.1007/s13143-014-0024-7, 2014.
815 Luoto, T. P., Oksman, M., and Ojala, A. E. K.: Climate change and bird impact as drivers of
816 High Arctic pond deterioration, Polar Biol, 38, 357-368, 10.1007/s00300-014-1592-9, 2015.
817 Lutz, S., Anesio, A. M., Villar, S. E. J., and Benning, L. G.: Variations of algal communities
818 cause darkening of a Greenland glacier, Fems Microbiol Ecol, 89, 402-414, 10.1111/1574-
819 6941.12351, 2014.
820 Lutz, S., Anesio, A. M., Edwards, A., and Benning, L. G.: Microbial diversity on Icelandic
821 glaciers and ice caps, Frontiers in microbiology, 6, ARTN 307
822 10.3389/fmicb.2015.00307, 2015.
823 Mapelli, F., Marasco, R., Rizzi, A., Baldi, F., Ventura, S., Daffonchio, D., and Borin, S.: Bacterial
824 Communities Involved in Soil Formation and Plant Establishment Triggered by Pyrite

825 Bioweathering on Arctic Moraines, Microbial Ecol, 61, 438-447, 10.1007/s00248-010-9758-
826 7, 2011.
827 McDonald, D., Price, M. N., Goodrich, J., Nawrocki, E. P., DeSantis, T. Z., Probst, A.,
828 Andersen, G. L., Knight, R., and Hugenholtz, P.: An improved Greengenes taxonomy with
829 explicit ranks for ecological and evolutionary analyses of bacteria and archaea, Isme J, 6,
830 610-618, 10.1038/ismej.2011.139, 2012.
831 Michelutti, N., Keatley, B. E., Brimble, S., Blais, J. M., Liu, H. J., Douglas, M. S. V., Mallory, M.
832 L., Macdonald, R. W., and Smol, J. P.: Seabird-driven shifts in Arctic pond ecosystems, P Roy
833 Soc B-Biol Sci, 276, 591-596, 10.1098/rspb.2008.1103, 2009.
834 Michelutti, N., Mallory, M. L., Blais, J. M., Douglas, M. S. V., and Smol, J. P.: Chironomid
835 assemblages from seabird-affected High Arctic ponds, Polar Biol, 34, 799-812,
836 10.1007/s00300-010-0934-5, 2011.
837 Mindl, B., Anesio, A. M., Meirer, K., Hodson, A. J., Laybourn-Parry, J., Sommaruga, R., and
838 Sattler, B.: Factors influencing bacterial dynamics along a transect from supraglacial runoff
839 to proglacial lakes of a high Arctic glacieri (vol 7, pg 307, 2007), Fems Microbiol Ecol, 59,
840 762-762, DOI 10.1111/j.1574-6941.2007.00295.x, 2007.
841 Moe, B., Stempniewicz, L., Jakubas, D., Angelier, F., Chastel, O., Dinessen, F., Gabrielsen, G.
842 W., Hanssen, F., Karnovsky, N. J., Ronning, B., Welcker, J., Wojczulanis-Jakubas, K., and Bech,
843 C.: Climate change and phenological responses of two seabird species breeding in the high-
844 Arctic, Mar Ecol Prog Ser, 393, 235-246, 10.3354/meps08222, 2009.
845 Moreau, M., Mercier, D., Laffly, D., and Roussel, E.: Impacts of recent paraglacial dynamics
846 on plant colonization: A case study on Midtre Lovenbreen foreland, Spitsbergen (79 degrees
847 N), Geomorphology, 95, 48-60, DOI 10.1016/j.geomorph.2006.07.031, 2008.
848 Moritz, R. E., Bitz, C. M., and Steig, E. J.: Dynamics of recent climate change in the Arctic,
849 Science, 297, 1497-1502, DOI 10.1126/science.1076522, 2002.
850 Oechel, W. C., Hastings, S. J., Vourlitis, G., Jenkins, M., Riechers, G., and Grulke, N.: Recent
851 Change of Arctic Tundra Ecosystems from a Net Carbon-Dioxide Sink to a Source, Nature,
852 361, 520-523, DOI 10.1038/361520a0, 1993.
853 Oechel, W. C., Vourlitis, G. L., Hastings, S. J., Zulueta, R. C., Hinzman, L., and Kane, D.:
854 Acclimation of ecosystem CO2 exchange in the Alaskan Arctic in response to decadal climate
855 warming, Nature, 406, 978-981, Doi 10.1038/35023137, 2000.
856 Paul, F., Frey, H., and Le Bris, R.: A new glacier inventory for the European Alps from Landsat
857 TM scenes of 2003: challenges and results, Ann Glaciol, 52, 144-152, 2011.
858 Prietzel, J., Dumig, A., Wu, Y. H., Zhou, J., and Klysubun, W.: Synchrotron-based P K-edge
859 XANES spectroscopy reveals rapid changes of phosphorus speciation in the topsoil of two
860 glacier foreland chronosequences, Geochim Cosmochim Ac, 108, 154-171, DOI
861 10.1016/j.gca.2013.01.029, 2013.
862 Schipper, L. A., Hobbs, J. K., Rutledge, S., and Arcus, V. L.: Thermodynamic theory explains
863 the temperature optima of soil microbial processes and high Q(10) values at low
864 temperatures, Global Change Biol, 20, 3578-3586, Doi 10.1111/Gcb.12596, 2014.
865 Schloss, P. D., Westcott, S. L., Ryabin, T., Hall, J. R., Hartmann, M., Hollister, E. B., Lesniewski,
866 R. A., Oakley, B. B., Parks, D. H., Robinson, C. J., Sahl, J. W., Stres, B., Thallinger, G. G., Van
867 Horn, D. J., and Weber, C. F.: Introducing mothur: Open-Source, Platform-Independent,
868 Community-Supported Software for Describing and Comparing Microbial Communities, Appl
869 Environ Microb, 75, 7537-7541, 10.1128/Aem.01541-09, 2009.
870 Schmidt, S. K., Reed, S. C., Nemergut, D. R., Grandy, A. S., Cleveland, C. C., Weintraub, M. N.,
871 Hill, A. W., Costello, E. K., Meyer, A. F., Neff, J. C., and Martin, A. M.: The earliest stages of

ecosystem succession in high-elevation (5000 metres above sea level), recently deglaciated soils, P Roy Soc B-Biol Sci, 275, 2793-2802, DOI 10.1098/rspb.2008.0808, 2008.

Schostag, M., Stibal, M., Jacobsen, C. S., Baelum, J., Tas, N., Elberling, B., Jansson, J. K., Semenchuk, P., and Prieme, A.: Distinct summer and winter bacterial communities in the active layer of Svalbard permafrost revealed by DNA- and RNA-based analyses, Frontiers in microbiology, 6, ARTN 399 10.3389/fmicb.2015.00399, 2015.

Schulz, S., Brankatschk, R., Dumig, A., Kogel-Knabner, I., Schloter, M., and Zeyer, J.: The role of microorganisms at different stages of ecosystem development for soil formation, Biogeosciences, 10, 3983-3996, DOI 10.5194/bg-10-3983-2013, 2013.

Schutte, U. M. E., Abdo, Z., Bent, S. J., Williams, C. J., Schneider, G. M., Solheim, B., and Forney, L. J.: Bacterial succession in a glacier foreland of the High Arctic, Isme J, 3, 1258-1268, DOI 10.1038/ismej.2009.71, 2009.

Scott, E. M., Rattray, E. A. S., Prosser, J. I., Killham, K., Glover, L. A., Lynch, J. M., and Bazin, M. J.: A Mathematical-Model for Dispersal of Bacterial Inoculants Colonizing the Wheat Rhizosphere, Soil Biol Biochem, 27, 1307-1318, Doi 10.1016/0038-0717(95)00050-O, 1995.

Serreze, M. C., Walsh, J. E., Chapin, F. S., Osterkamp, T., Dyurgerov, M., Romanovsky, V., Oechel, W. C., Morison, J., Zhang, T., and Barry, R. G.: Observational evidence of recent change in the northern high-latitude environment, Climatic Change, 46, 159-207, Doi 10.1023/A:1005504031923, 2000.

Simon, M., and Azam, F.: Protein-Content and Protein-Synthesis Rates of Planktonic Marine-Bacteria, Mar Ecol Prog Ser, 51, 201-213, DOI 10.3354/meps051201, 1989.

Smittenberg, R. H., Gierga, M., Goransson, H., Christl, I., Farinotti, D., and Bernasconi, S. M.: Climate-sensitive ecosystem carbon dynamics along the soil chronosequence of the Damma glacier forefield, Switzerland, Global Change Biol, 18, 1941-1955, DOI 10.1111/j.1365-2486.2012.02654.x, 2012.

Soetaert, K., and Herman, P.: A Practical Guide to Ecological Modelling: Using R as a Simulation Platform, Springer, UK, 2009.

Staines, K. E. H., Carrivick, J. L., Tweed, F. S., Evans, A. J., Russell, A. J., Jóhannesson, T., and Roberts, M.: A multi-dimensional analysis of pro-glacial landscape change at Sólheimajökull, southern Iceland, Earth Surface Processes and Landforms, 40, 809-822, 10.1002/esp.3662, 2014.

Stapleton, L. M., Crout, N. M. J., Sawstrom, C., Marshall, W. A., Poulton, P. R., Tye, A. M., and Laybourn-Parry, J.: Microbial carbon dynamics in nitrogen amended Arctic tundra soil: Measurement and model testing, Soil Biol Biochem, 37, 2088-2098, DOI 10.1016/j.soilbio.2005.03.016, 2005.

Stibal, M., Tranter, M., Benning, L. G., and Rehak, J.: Microbial primary production on an Arctic glacier is insignificant in comparison with allochthonous organic carbon input, Environ Microbiol, 10, 2172-2178, 10.1111/j.1462-2920.2008.01620.x, 2008.

Strauss, S. L., Garcia-Pichel, F., and Day, T. A.: Soil microbial carbon and nitrogen transformations at a glacial foreland on Anvers Island, Antarctic Peninsula, Polar Biol, 35, 1459-1471, DOI 10.1007/s00300-012-1184-5, 2012.

Telling, J., Anesio, A. M., Tranter, M., Irvine-Fynn, T., Hodson, A., Butler, C., and Wadham, J.: Nitrogen fixation on Arctic glaciers, Svalbard, J Geophys Res-Biogeo, 116, Artn G03039 Doi 10.1029/2010jg001632, 2011.

Telling, J., Stibal, M., Anesio, A. M., Tranter, M., Nias, I., Cook, J., Bellas, C., Lis, G., Wadham, J. L., Sole, A., Nienow, P., and Hodson, A.: Microbial nitrogen cycling on the Greenland Ice Sheet, Biogeosciences, 9, 2431-2442, 10.5194/bg-9-2431-2012, 2012.

Toal, M. E., Yeomans, C., Killham, K., and Meharg, A. A.: A review of rhizosphere carbon flow modelling, Plant Soil, 222, 263-281, Doi 10.1023/A:1004736021965, 2000.

Tscherko, D., Rustemeier, J., Richter, A., Wanek, W., and Kandeler, E.: Functional diversity of the soil microflora in primary succession across two glacier forelands in the Central Alps, Eur J Soil Sci, 54, 685-696, DOI 10.1046/j.1365-2389.2003.00570.x, 2003.

Vandewerf, H., and Verstraete, W.: Estimation of Active Soil Microbial Biomass by Mathematical-Analysis of Respiration Curves - Development and Verification of the Model, Soil Biol Biochem, 19, 253-260, Doi 10.1016/0038-0717(87)90006-X, 1987.

Yde, J. C., Finster, K. W., Raiswell, R., Steffensen, J. P., Heinemeier, J., Olsen, J., Gunnlaugsson, H. P., and Nielsen, O. B.: Basal ice microbiology at the margin of the Greenland ice sheet, Ann Glaciol, 51, 71-79, 2010.

Yoshitake, S., Uchida, M., Koizumi, H., Kanda, H., and Nakatsubo, T.: Production of biological soil crusts in the early stage of primary succession on a High Arctic glacier foreland, New Phytol, 186, 451-460, DOI 10.1111/j.1469-8137.2010.03180.x, 2010.

Zdanowski, M. K., Zmuda-Baranowska, M. J., Borsuk, P., Swiatecki, A., Gorniak, D., Wolicka, D., Jankowska, K. M., and Grzesiak, J.: Culturable bacteria community development in postglacial soils of Ecology Glacier, King George Island, Antarctica, Polar Biol, 36, 511-527, DOI 10.1007/s00300-012-1278-0, 2013.

Zelenev, V. V., van Bruggen, A. H. C., and Semenov, A. M.: "BACWAVE," a spatial-temporal model for traveling waves of bacterial populations in response to a moving carbon source in soil, Microbial Ecol, 40, 260-272, 2000.

Zhang, X. Y., Wang, W., Chen, W. L., Zhang, N. L., and Zeng, H.: Comparison of Seasonal Soil Microbial Process in Snow-Covered Temperate Ecosystems of Northern China, Plos One, 9, ARTN e92985
10.1371/journal.pone.0092985, 2014.

Ziolek, M., and Melke, J.: The impact of seabirds on the content of various forms of phosphorus in organic soils of the Bellsund coast, western Spitsbergen, Polar Res, 33, ARTN 19986
10.3402/polar.v33.19986, 2014.

Zumsteg, A., Bernasconi, S. M., Zeyer, J., and Frey, B.: Microbial community and activity shifts after soil transplantation in a glacier forefield, Appl Geochem, 26, S326-S329, DOI 10.1016/j.apgeochem.2011.03.078, 2011.

Zumsteg, A., Luster, J., Goransson, H., Smittenberg, R. H., Brunner, I., Bernasconi, S. M., Zeyer, J., and Frey, B.: Bacterial, Archaeal and Fungal Succession in the Forefield of a Receding Glacier, Microbial Ecol, 63, 552-564, DOI 10.1007/s00248-011-9991-8, 2012.

Zumsteg, A., Schmutz, S., and Frey, B.: Identification of biomass utilizing bacteria in a carbon-depleted glacier forefield soil by the use of 13C DNA stable isotope probing, Env Microbiol Rep, 5, 424-437, Doi 10.1111/1758-2229.12027, 2013.

Biogeosciences Discuss., doi:10.5194/bg-2016-52, 2016
Manuscript under review for journal Biogeosciences
Published: 16 February 2016

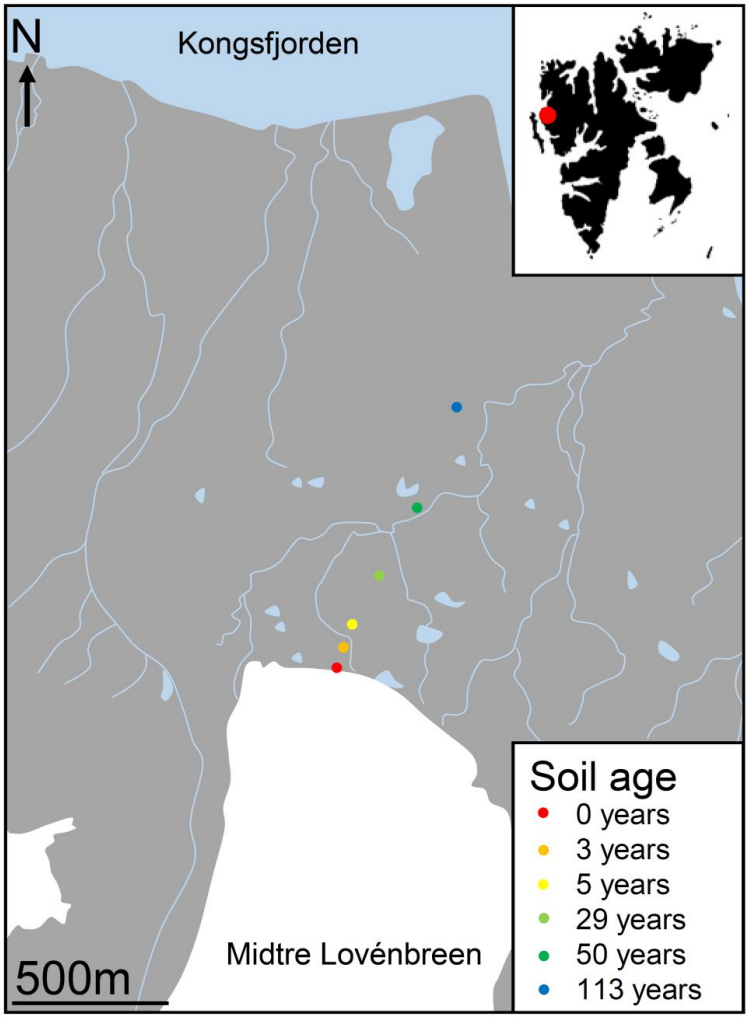

966
967 Figure 1. Midtre Lovénbreen glacier and forefield in Svalbard, the location of sampling sites and
968 approximate age of soil.
969

Biogeosciences Discuss., doi:10.5194/bg-2016-52, 2016
Manuscript under review for journal Biogeosciences
Published: 16 February 2016

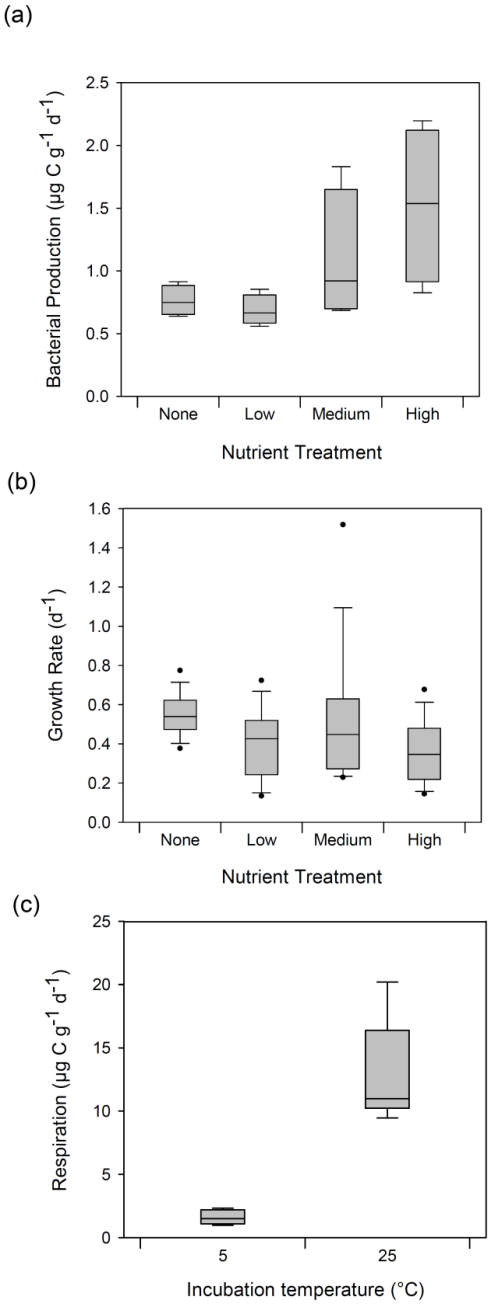

Figure 2. Measurements of (a) bacterial carbon production and (b) growth rate, derived from ^{3}H-leucine assays at different nutrient conditions, and (c) bacterial respiration at 5˚C and 25˚C.

Biogeosciences Discuss., doi:10.5194/bg-2016-52, 2016
Manuscript under review for journal Biogeosciences
Published: 16 February 2016

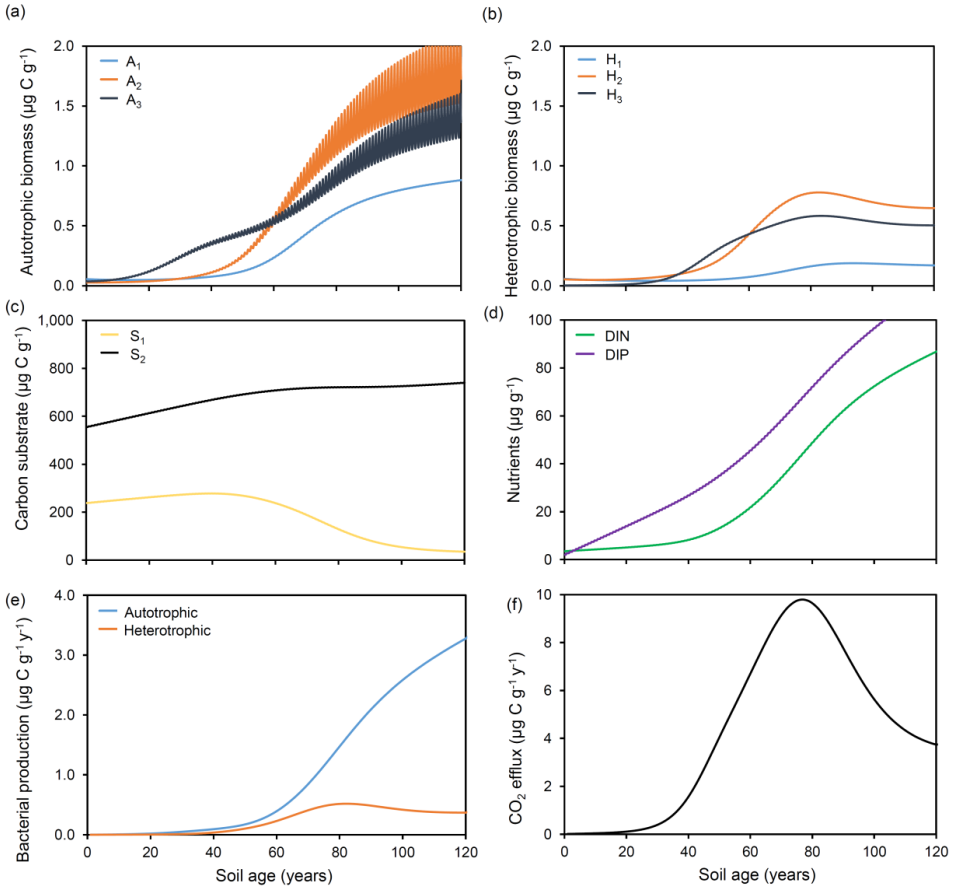

Figure 3. Modelled (a) autotrophic biomass, (b) heterotrophic biomass, (c) carbon substrate, (d) nutrients, (e) bacterial production and (f) CO_2 efflux, with laboratory-derived parameter values.

Biogeosciences Discuss., doi:10.5194/bg-2016-52, 2016
Manuscript under review for journal Biogeosciences
Published: 16 February 2016

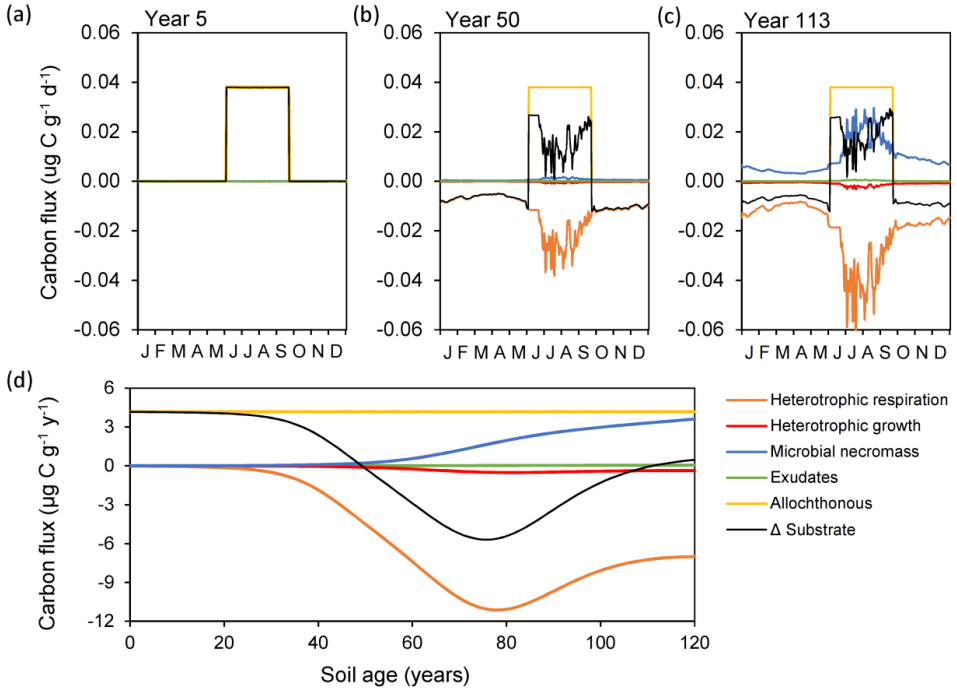

Figure 4. Illustration of daily carbon fluxes for (a) 5, (b) 50 and (c) 113 year old soil, and (d) annual carbon flux over 120 years. Microbial necromass (blue), exudates (green) and allochthonous sources (yellow) contribute to the substrate pool (black), and heterotrophic growth (red) and respiration (orange) deplete it.

Biogeosciences Discuss., doi:10.5194/bg-2016-52, 2016
Manuscript under review for journal Biogeosciences
Published: 16 February 2016

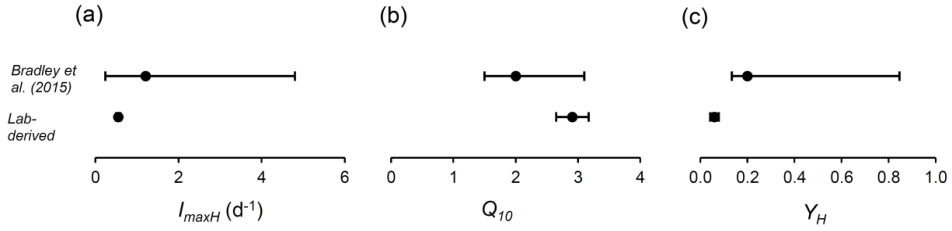

Figure 5. A comparison of previously established ranges for parameters (Bradley et al., 2015) with laboratory-derived values for (a) maximum growth rate (I_{max}), (b) temperature response (Q_{10}), (c) BGE (Y).

Biogeosciences Discuss., doi:10.5194/bg-2016-52, 2016
Manuscript under review for journal Biogeosciences
Published: 16 February 2016

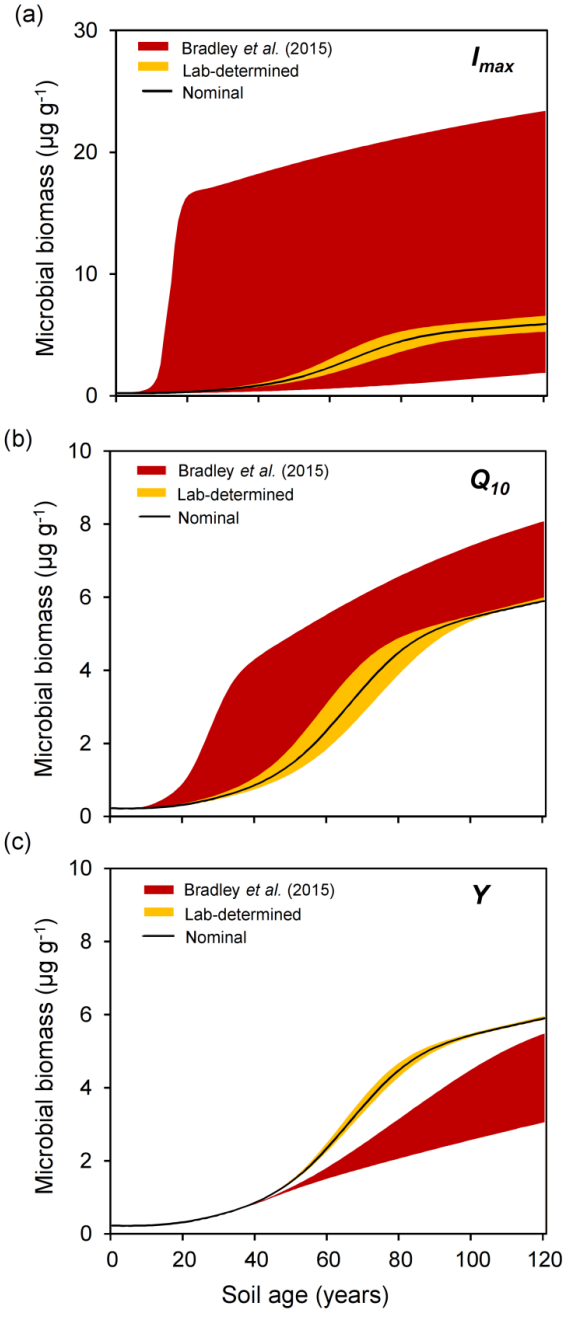

990

991 Figure 6. A comparison of predicted microbial biomass with laboratory-derived parameter values
992 (yellow) and previously established parameter values (Bradley et al., 2015) (red) for variation in the
993 following parameters: (a) maximum growth rate (I_{max}), (b) temperature response (Q_{10}), (c) BGE (Y).

994

Biogeosciences Discuss., doi:10.5194/bg-2016-52, 2016
Manuscript under review for journal Biogeosciences
Published: 16 February 2016

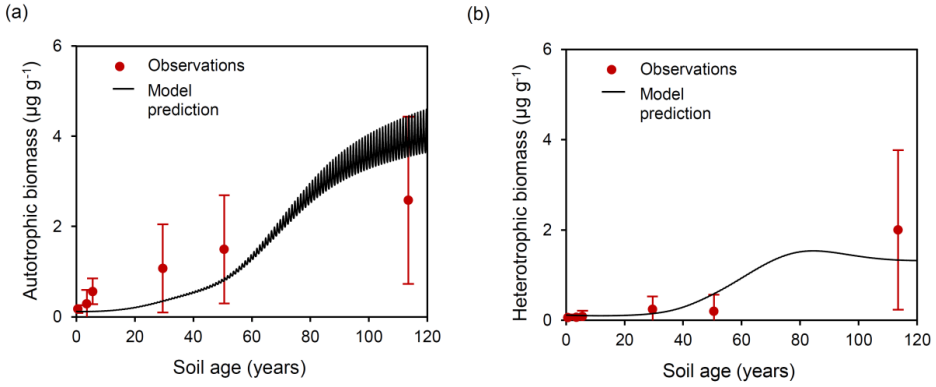

995
996 Figure 7. Model predictions of (a) autotrophic and (b) heterotrophic biomass (black line), compared to
997 observational data (red) derived from microscopy.
998

Biogeosciences Discuss., doi:10.5194/bg-2016-52, 2016
Manuscript under review for journal Biogeosciences
Published: 16 February 2016

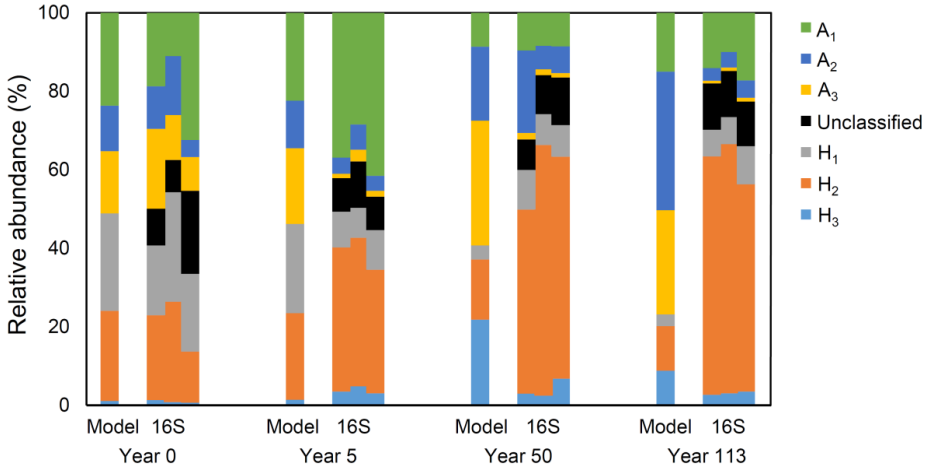

Figure 8. A comparison of microbial diversity from model output and genomic analyses at 0 year old, 5 year old, 50 year old and 113 year old soil.

Biogeosciences Discuss., doi:10.5194/bg-2016-52, 2016
Manuscript under review for journal Biogeosciences
Published: 16 February 2016

1005
1006 Table 1. State variables and initial values.

State Variable	Units	Description	Initial value (year 0) (μg g^{-1})
A_1	μg C g^{-1}	Subglacial chemolithoautotrophs	*0.0547*
A_2	μg C g^{-1}	Soil autotrophs	*0.0266*
A_3	μg C g^{-1}	Nitrogen fixing soil autotrophs	*0.0355*
H_1	μg C g^{-1}	Subglacial heterotrophs	*0.0576*
H_2	μg C g^{-1}	Soil heterotrophs	*0.0530*
H_3	μg C g^{-1}	Nitrogen fixing soil heterotrophs	*0.0025*
S_1	μg C g^{-1}	Labile organic carbon	*291.895*
S_2	μg C g^{-1}	Refractory organic carbon	*681.089*
DIN	μg N g^{-1}	Dissolved inorganic nitrogen (DIN)	*3.530*
DIP	μg P g^{-1}	Dissolved inorganic phosphorus (DIP)	*2.078*
ON_1	μg N g^{-1}	Labile organic nitrogen	*41.157*
ON_2	μg N g^{-1}	Refractory organic nitrogen	*96.034*
OP_1	μg P g^{-1}	Labile organic phosphorus	*24.227*
OP_2	μg P g^{-1}	Refractory organic phosphorus	*56.530*

1007
1008
1009
1010

Biogeosciences Discuss., doi:10.5194/bg-2016-52, 2016
Manuscript under review for journal Biogeosciences
Published: 16 February 2016

1011 Table 2. Microbial biomass in the forefield of Midtre Lovénbreen (brackets show 1 standard deviation)
1012

Soil Age (years)	Autotrophic biomass (µg C g^{-1})		Heterotrophic biomass (µg C g^{-1})		Total Organic Carbon (µg C g^{-1})	
0	0.171	(0.042)	0.059	*(0.034)*	792.984	(127.206)
3	0.287	(0.155)	0.064	*(0.029)*		
5	0.561	(0.143)	0.083	*(0.065)*		
29	1.072	(0.487)	0.244	*(0.142)*		
50	1.497	(0.601)	0.197	*(0.184)*		
113	2.581	(0.927)	2.000	*(0.885)*		

1013
1014
1015
1016
1017
1018

Biogeosciences Discuss., doi:10.5194/bg-2016-52, 2016
Manuscript under review for journal Biogeosciences
Published: 16 February 2016

1019 Table 3. Model output.

Soil Age (years)	Autotrophic biomass (µg C g^{-1})	Heterotrophic biomass (µg C g^{-1})	Autotrophic production (µg C g^{-1} y^{-1})	Heterotrophic production (µg C g^{-1} y^{-1})	Net CO_2 efflux (µg C g^{-1} y^{-1})	DIN assimilation (µg N g^{-1} y^{-1})	N_2 fixation (µg N g^{-1} y^{-1})
0	0.117	0.111	0.002	0.001	0.011	2.0×10^{-4}	2.0×10^{-4}
3	0.117	0.105	0.003	0.001	0.020	3.0×10^{-4}	3.0×10^{-4}
5	0.119	0.102	0.004	0.001	0.025	4.0×10^{-4}	4.0×10^{-4}
29	0.359	0.147	0.050	0.012	0.391	0.002	0.006
50	0.860	0.591	0.187	0.113	4.311	0.022	0.021
113	4.414	1.331	3.093	0.376	4.031	0.458	0.031

1020
1021
1022
1023
1024
1025
1026